



Sediment storage and release from Himalayan piggyback basins and implications for downstream river morphology and evolution

Journal:	<i>Basin Research</i>
Manuscript ID:	BRE-070-2014.R1
Manuscript Type:	Original Article
Date Submitted by the Author:	n/a
Complete List of Authors:	Densmore, Alexander; Durham University, Department of Geography; Sinha, R.; IIT Kanpur, Earth Sciences Sinha, Swati; IIT Kanpur, Earth Sciences Tandon, S.K.; IIT Kanpur, Earth Sciences Jain, Vikrant; IIT Gandhinagar, Earth Sciences
Keywords:	foreland basins, sediment flux, tectonics and sedimentation

SCHOLARONE™
Manuscripts

1 **1 Sediment storage and release from Himalayan piggyback basins and implications for downstream river**
2
3 **2 morphology and evolution**
4

5
6
7
8 Alexander L. Densmore^{1*}, Rajiv Sinha², Swati Sinha², S.K. Tandon², and Vikrant Jain³
9

10 ¹ Institute of Hazard, Risk and Resilience and Department of Geography, Durham University, Durham DH1
11
12 3LE, UK
13

14 ² Department of Earth Sciences, Indian Institute of Technology Kanpur, Kanpur 208016 (UP), India
15

16 ³ Division of Earth Sciences, Indian Institute of Technology Gandhinagar, Ahmedabad 382424, Gujarat, India
17

18 * Corresponding author: email a.l.densmore@dur.ac.uk
19
20
21
22

23 **11 Abstract**
24

25 Piggyback basins developed at the mountain fronts of collisional orogens can act as important, and
26
27 transient, sediment stores along major river systems. It is not clear, however, how the storage and release
28
29 of sediment in piggyback basins affects the sediment flux and evolution of downstream river reaches. Here
30
31 we investigate the timing and volumes of sediment storage and release in the Dehra Dun, a piggyback basin
32
33 developed along the Himalayan mountain front in northwestern India. Based on OSL dating, we show
34
35 evidence for three major phases of aggradation in the dun, bracketed at ~41-33 ka, 34-21 ka, and 23-10 ka,
36
37 each accompanied by progradation of sediment fans into the dun. Each of these phases was followed by
38
39 backfilling and (apparently) rapid fan-head incision, leading to abandonment of the depositional unit and a
40
41 basinward shift of the active depocentre. Excavation of dun sediment after the second and third phases of
42
43 aggradation produced time-averaged sediment discharges that were ~1-2% of the modern suspended-
44
45 sediment discharges of the Ganga and Yamuna rivers that traverse the margins of the dun; this sediment is
46
47 derived from catchment areas that together comprise 1.5% of the drainage area of these rivers.
48
49 Comparison of the timing of dun storage and release with upstream and downstream records of incision
50
51 and aggradation in the Ganga show that sediment storage in the dun generally coincides with periods of
52
53 widespread hinterland aggradation but that late stages of dun aggradation, and especially times of dun
54
55 sediment excavation, coincide with major periods of sediment export to the Ganga Basin. The dun thus acts
56
57
58
59
60

1
2 28 to amplify temporal variations in hinterland sediment supply or transport capacity. This conceptual model
3
4 29 appears to explain morphological features of other major river systems along the Himalayan front,
5
6 30 including the Gandak and Kosi Rivers, and may be important for understanding sediment flux variations in
7
8 31 other collisional mountain belts.
9

10 32

11
12 33 **Keywords**

13
14 34 Himalayas, Ganga River basin, sediment transport, sediment storage, erosion, intermontane valley
15
16
17
18
19
20
21
22
23
24
25
26
27
28
29
30
31
32
33
34
35
36
37
38
39
40
41
42
43
44
45
46
47
48
49
50
51
52
53
54
55
56
57
58
59
60

1
2 35 **Introduction**

3
4 36 Piggyback basins are ubiquitous features of foreland basin systems (Ori and Friend, 1984; DeCelles and
5
6 37 Giles, 1996), and serve as links between hinterland areas of sediment production and foreland
7
8 38 depocentres. While such basins may be essentially passive features that fill with sediment and then are
9
10 39 buried as the fold and thrust belt migrates into the foreland (e.g., DeCelles and Horton, 2003), several
11
12 40 studies have shown that piggyback basins may be highly dynamic environments on shorter time scales (10^3
13
14 41 – 10^4 years), with repeated cycles of aggradation and incision (e.g., DeCelles et al., 1991; Hilley and
15
16 42 Strecker, 2005). Temporary trapping and release of sediment in piggyback basins or other intermediate
17
18 43 sediment stores is thus a critical control on long-term sediment efflux, not least because such storage can
19
20 44 buffer the system against changes in external forcing conditions (Castelltort and van den Driessche, 2003).
21
22

23 45
24
25 46 It has long been known that intermediate storage can account for a large proportion of the sediment
26
27 47 produced in upstream parts of a catchment (e.g., Meade, 1982; Walling, 1983; Phillips, 1991; Blum and
28
29 48 Törnqvist, 2000; Bloethe and Korup, 2013), but our understanding of the downstream impacts of sediment
30
31 49 storage and release remains relatively limited. These impacts have been investigated in analogue
32
33 50 experiments (e.g., Kim et al., 2006; Powell et al., 2012) and numerical simulations (Paola, 2000; Allen and
34
35 51 Densmore, 2000; Carretier and Lucazeau, 2005), or at relatively small spatial scales (e.g., Lane and Richards,
36
37 52 1997; Malmon et al., 2005; Lancaster and Casebeer, 2007), but field examples in large river systems are
38
39 53 comparatively scarce (e.g., Clift, 2006).
40
41
42

43 54
44
45 55 Here, we begin to address this problem by focusing on sediment storage and release along the Himalayan
46
47 56 mountain front, portions of which are characterized by frontal piggyback basins or ‘duns’ along individual
48
49 57 segments of the mountain front (Nakata, 1972; Raiverman, 1997; Powers et al., 1998; Thakur and Pandey,
50
51 58 2004; Thakur et al., 2007). These duns are formed in response to marked along-strike variations in the
52
53 59 geometry and distribution of slip on the Himalayan Frontal Thrust (HFT) system (Nakata, 1989; Yeats et al.,
54
55 60 1992; Wesnousky et al., 1999; Thakur, 2013). Some of the main Himalayan river systems – including the
56
57 61 Yamuna, Ganga, and Gandak – flow across these duns before debouching into the foreland basin, whereas
58
59
60

1
2 62 others – including the Ghaghra, Karnali, and Kosi – flow directly into the foreland (Fig. 1). This region thus
3
4 63 provides an opportunity to assess the rates and timing of sediment storage and evacuation from the duns,
5
6 64 the role of duns in setting sediment supply to the foreland, and the effects of the presence or absence of a
7
8 65 dun on the geomorphology of large Himalayan river systems.
9

10 66

11
12 67 We focus initially on the Dehra Dun in northwestern India, which is traversed by two of the largest rivers of
13
14 68 the Ganga Basin, the Yamuna and Ganga rivers. We use this example to examine the degree to which
15
16 69 proximal piggyback basins can influence the timing and magnitude of sediment discharge in a large river
17
18 70 system. Ray and Srivastava (2010) provided a comprehensive review of the evidence for aggradation and
19
20 71 incision in the mountain hinterland of the Ganga Basin upstream of the Dehra dun, and linked this with
21
22 72 downstream records of sediment accumulation and incision in the Ganga plain. Our work fills the gap
23
24 73 between these regions, and allows us to evaluate the role of the dun in the Ganga sediment routing
25
26 74 system. We combine new and published data on the geometry and age of sedimentary deposits in the dun
27
28 75 into a conceptual model of dun evolution since ~40 ka. We use this model to estimate the volumes of
29
30 76 sediment that have been stored and released over this time period, and to compare events in the dun with
31
32 77 episodes of aggradation and incision that have been documented for the Ganga and Yamuna rivers in the
33
34 78 hinterland (Ray and Srivastava, 2010) and foreland (e.g., Gibling et al., 2011; Roy et al., 2012). Finally, we
35
36 79 evaluate the conceptual model against observations from the Gandak and Kosi Rivers, and show that
37
38 80 fundamental differences in the foreland morphology and evolution of foreland rivers can be linked to the
39
40 81 presence or absence of a dun sediment store.
41
42
43
44

45 82

46 83 **Study area**

47 84 *Setting*

48
49 85 The development of duns along some, but not all, segments of the Himalayan mountain front (Fig. 1) has
50
51 86 been linked to a number of different factors, including structures on the underlying Indian lithosphere
52
53 87 (Yeats and Lillie, 1991; Raiverman et al., 1993) or lateral variations in orogenic wedge properties (Mugnier
54
55 88 et al., 1999a, 1999b), leading to differences in the extent to which strands of the HFT have propagated into
56
57
58
59
60

1
2 89 the foreland. For example, Mugnier et al. (1999b) showed that thicker Siwalik deposits and a slightly
3
4 90 steeper (2°) dip of the basal detachment would produce early propagation of the thrust front and thus
5
6 91 large stable wedge-top or piggyback basins. They suggested that the Dehra and Chitwan duns might form
7
8 92 via a similar mechanism. More generally, Leturmy et al. (2000) argued that erosion or deposition of the
9
10 93 wedge could promote or suppress piggyback basin development, by controlling the timing and propagation
11
12 94 of faulting into the foreland. Simpson (2010), in contrast, demonstrated that the strength of the basal
13
14 95 detachment, and to a lesser extent the strength of the cover sequence, controls the sequence and
15
16 96 propagation of deformation. A frictional (high-viscosity) detachment leads to regular propagation of the
17
18 97 wedge and localization of deformation at the thrust front. A weak detachment, in contrast, leads to rapid
19
20 98 propagation of slip into the foreland and formation of wedge-top basins, but activity on individual faults is
21
22 99 episodic and deformation shifts frequently from the thrust front to structures in the hinterland. What is
23
24 100 important for our purposes is that dun development is spatially limited along the Himalayan front, and
25
26 101 affects only some of the major Himalayan rivers (Fig. 1).
27
28
29

102

103 *The Dehra Dun*

104 The Dehra Dun (Fig. 2), in Uttarakhand state, northern India, has developed in response to folding of the
105 Mohand anticline over a ramp in the HFT, which has remained active into the Holocene (Wesnousky et al.,
106 1999). The anticline is an upright, asymmetric fold composed of Middle and Upper Siwalik sandstones and
107 conglomerates of Miocene to Pleistocene age; the onset of folding and dun formation is constrained to
108 after ~ 500 ka but before 220 ka (Thakur et al., 2007; Barnes et al., 2011). Accommodation generation in the
109 dun is controlled by slip on both the HFT and the Main Boundary Thrust (MBT) (Fig. 2).
110

111

112 The Yamuna and Ganga rivers traverse the lateral margins of the dun before entering the foreland, and set
113 base level for the channels that drain the dun. Thus, any storage or erosion of sediments in the dun has a
114 direct impact on the sediment discharge of the Yamuna and Ganga rivers at the HFT. A complex late-
115 Quaternary history of aggradation and erosion within the dun is recorded by sequences of fill terraces along
both the Yamuna (Dutta et al., 2012) and Ganga (Sinha et al., 2010). The Yamuna terraces in the footwall of

1
2 116 the MBT (Fig. 2) record major phases of aggradation from >37 to 24 ka and >15 to 12 ka, each followed by
3
4 117 incision and terrace abandonment, along with several minor aggradation and incision cycles within the
5
6 118 Holocene (Dutta et al., 2012). The Ganga terraces span a shorter time period, but also record aggradation
7
8 119 to ~11 ka followed by incision from 11-9.7 ka (Sinha et al., 2010). These records are matched by evidence
9
10 120 from fill terraces at a number of upstream sites in the Ganga Basin, which broadly indicate phases of
11
12 121 aggradation from ~49-25 ka and ~18-11 ka, with incision beginning soon after 11 ka (Srivastava et al., 2008;
13
14 122 Ray and Srivastava, 2010).
15
16 123
17
18 124 Sediment supply from the Ganga and Yamuna rivers at the Himalayan mountain front, or alternatively the
19
20 125 hinterland erosion rates of these basins, has been quantified over several different time scales. Jha et al.
21
22 126 (1988) used measurements of suspended sediment for a single year to estimate a present-day suspended
23
24 127 sediment discharge for the Yamuna of 18 Mt/yr at Tajewala, just downstream of the HFT; assuming a solid
25
26 128 grain density of 2650 kg/m³, this corresponds to a volumetric discharge of 6.8 Mm³/yr. Lupker et al. (2012)
27
28 129 used cosmogenic radionuclide analysis of a bed sample from Paonta, within the dun, to estimate a total
29
30 130 sediment discharge of 13±5 Mt/yr or 5.3 Mm³/yr. Values for the Ganga vary more widely. Reported
31
32 131 present-day discharge estimates from suspended sediment measurements at Rishikesh or Haridwar are 13-
33
34 132 14 Mt/yr (Abbas and Subramian, 1984; Sinha et al., 2005; Chakrapani and Saini, 2009), and Wasson (2003)
35
36 133 cited a value of 33 Mt/yr on the basis of Galy and France-Lanord (2001), but further supporting analysis is
37
38 134 not available for this estimate. These correspond to volumetric discharges of ~5 Mm³/yr. In contrast, Vance
39
40 135 et al. (2003) and Lupker et al. (2012) used cosmogenic radionuclides to derive longer-term Ganga sediment
41
42 136 discharge estimates of 20-30 Mm³/yr (or 65-67 Mt/yr) and 52 Mm³/yr (or 139±37 Mt/yr), respectively.
43
44 137
45
46 138 Sediment is also supplied to the dun, and thus to the Yamuna and Ganga rivers, by a set of catchments that
47
48 139 drain the hanging wall of the MBT (Fig. 2), with a total area of about 503 km² upstream of the MBT; this
49
50 140 represents about 1.5% of the total catchment area of the Yamuna and Ganga upstream of the HFT (34,300
51
52 141 km²). These dun catchments feed a set of coalescing stream-flow and debris-flow fans that have deposited
53
54 142 a thick sequence of sediment, ranging from silts to cobble conglomerates, atop Upper Siwalik bedrock
55
56
57
58
59
60

1
2 143 (Singh et al., 2001). At the northern edge of the dun, Middle Siwalik rocks are folded and thrust over the fan
3
4 144 deposits (Thakur et al., 2007), while the youngest generation of fan deposits have backfilled paleovalleys
5
6 145 eroded into the hanging walls of the Santaugarh fault and the MBT (Fig 2). Nossin (1971) and Nakata (1972)
7
8 146 mapped the sedimentary fill of the Dehra Dun, and classified it into several discrete fan and terrace units.
9
10 147 Singh et al. (2001) extended this classification and identified three main depositional fans within the dun;
11
12 148 from west to east, these are the Donga, Dehradun, and Bhogpur fans (Fig. 2) and we adopt this
13
14 149 nomenclature here.

150

151

152 **Methods**

153 To assess sediment volumes and storage in the dun, we prepared geomorphic maps of the central Dehra
154 Dun showing the major fan surfaces and fill terraces, using LISS-3 satellite images (23.5 m spatial resolution)
155 from 2004 and the CGIAR-CSI Shuttle Radar Topography Mission version 4 digital elevation model (DEM),
156 with a cell size of 90 m. False-colour composite images were prepared from the LISS-3 data, using near-
157 infrared, red, and green bands. Identification and correlation of different fan and terrace surfaces was done
158 on the basis of the false-colour composite images, a Normal Difference Vegetation Index (NDVI) image
159 created from the LISS-3 data, the DEM, and a gradient raster created from the DEM. We also obtained a
160 total of 118 borehole logs from Uttar Pradesh Jal Nigam for locations within the dun in order to map the
161 major lithological transitions and establish minimum fan deposit thicknesses. In addition, field data on
162 elevations of the Quaternary surfaces and exposed Siwalik bedrock were collected using handheld GPS and
163 1:50,000 Survey of India topographic maps. Stratigraphic logs were prepared to characterise the sub-
164 surface deposits of most of the mapped geomorphic surfaces. We collected six samples for optically-
165 stimulated luminescence (OSL) dating from beds of fine to very fine sand and coarse silt within the fan
166 deposits (see Supplementary Material for methods and analytical procedures). These data were integrated
167 with the geomorphic maps and with existing OSL dates (Singh et al., 2001; Thakur et al., 2007) to constrain
168 the timing and geometry of major aggradational episodes in the dun.

169

1
2 170 To assess the contribution of dun sediment storage and evacuation to the Yamuna and Ganga Rivers, we
3
4 171 estimated the volumes of the major depositional units, and of the material that was removed from each
5
6 172 unit by incision. To do this, we correlated remnant depositional surfaces across the fans using elevation,
7
8 173 surface morphology and image texture, vegetation, and available OSL age constraints. We then
9
10 174 interpolated smooth surfaces across the correlated remnants using polynomial functions in ArcGIS. These
11
12 175 surfaces were constrained to include the mapped remnants, and were truncated where they dipped below
13
14 176 older, higher topography (either bedrock or older depositional units); we also ensured that the interpolated
15
16 177 surfaces were bounded by the MBT and by the present-day boundaries of the fans. By subtracting the
17
18 178 interpolated surfaces from the present-day topography, we estimated the depth and spatial pattern of
19
20 179 post-abandonment incision into each surface, which can be summed to yield the volume of sediment that
21
22 180 was removed during abandonment. We compared the results of interpolations using third, fourth, and
23
24 181 fifth-order polynomials, and found that the estimated volumes differed by $\leq 5\%$, so only results using
25
26 182 fourth-order polynomial interpolations are reported below. We also checked our incision patterns against
27
28 183 minimum sediment fill thicknesses from the borehole logs, to ensure that the estimates were geologically
29
30 184 reasonable and did not exceed the present-day sediment thicknesses along the valley floors. The volume
31
32 185 estimates assume that previous episodes of incision did not lower thalweg elevations in the dun below
33
34 186 present-day elevations, and are thus minima; however, we lack any evidence of the depth of incision or
35
36 187 clear subsurface distinctions between different depositional units, so at present this limitation cannot be
37
38 188 addressed. Finally, we combined our volumes of sediment removal with the time constraints provided by
39
40 189 the OSL dates to estimate average sediment discharges out of the dun.
41
42
43
44
45
46

190

191 **Results**

192 *Geometry and timing of depositional units*

193 Because the detailed stratigraphy of the sedimentary fill in the Dehra Dun has been described by Singh et
194 al. (2001), we focus here on the geometry and ages of the deposits. We concentrate on the most
195 volumetrically important depositional units that comprise the Donga, Dehradun, and Bhogpur fans, and
196 ignore both the younger, more spatially-restricted fill terrace deposits along streams in the dun (Nakata,
197
198
199
200

1
2 197 1972) and the older deposits in the hanging wall of the Santaugarh fault (the 'Dissected Siwalik Hills' of
3
4 198 Singh et al., 2001), which clearly pre-date the formation of the present-day dun. From oldest to youngest,
5
6 199 these key depositional units (Fig. 2) are here termed (1) the 'isolated hills' unit, which corresponds to the
7
8 200 'Pedimented Siwalik Hills' geomorphic unit and depositional unit GD-I of Singh et al. (2001), and unit A of
9
10 201 Thakur et al. (2007); (2) the 'proximal fan' unit, which corresponds to the Piedmont geomorphic unit and
11
12 202 depositional unit GD-II of Singh et al. (2001), and unit B of Thakur et al. (2007); and (3) the 'distal fan' unit,
13
14 203 which corresponds to depositional units GD-III and GD-IV of Singh et al. (2001), and unit C of Thakur et al.
15
16 204 (2007).
17
18
19 205

20
21 206 The isolated hills unit is composed of massive, clast- or matrix-supported pebble to boulder conglomerates
22
23 207 (Singh et al., 2001). These deposits form rounded hills that reach elevations of 620-880 m that flank the
24
25 208 major dun rivers (Sitla Rao, the Suarna River, and the Asan River) in the western and central parts of the
26
27 209 dun (Fig. 2, 3). Exposure of this unit is limited to a narrow belt, 2-4 km wide, in the immediate footwall of
28
29 210 the Santaugarh fault. The exposed thickness is at least 90 m, but the actual thickness of this unit is
30
31 211 unknown. Singh et al. (2001) inferred a basal age of ~50 ka based on OSL ages of 40.3 ± 3.9 and 38.3 ± 9.4 ka
32
33 212 near the base of this unit on the Dehradun fan, and also reported an age of 29.5 ± 5.0 ka from the Donga
34
35 213 fan, although its position is not certain. Thakur et al. (2007) reported OSL ages of 35.40 ± 7.30 and
36
37 214 33.57 ± 4.73 ka from this unit, both from proximal parts of the Donga fan. Our sample IH/2 yields an age of
38
39 215 41.3 ± 1.2 ka from 2.8 m below the top of an exposure of isolated hills sediment on the east flank of the
40
41 216 Suarna River valley (Fig. 2, Table 1).
42
43
44
45 217

46
47 218 The proximal fan unit consists of massive, clast- or matrix-supported pebble to boulder conglomerates with
48
49 219 some interbedded sand layers (Singh et al., 2001; Thakur et al., 2007). The unit underlies smooth, south-
50
51 220 dipping near-planar fan surfaces (Fig. 3A) that cover most of the proximal areas of the Donga, Dehradun,
52
53 221 and Bhogpur fans (Fig. 2), and extend 5-10 km downstream of the Santaugarh fault (for the Donga and
54
55 222 Dehradun fans) or the MBT (for the Bhogpur fan). These fan surfaces have typical surface slopes (averaged
56
57 223 over 270 m windows) of 2-4 degrees, and appear to onlap onto deposits of the underlying isolated hills in
58
59
60

1
2 224 the footwall of the Santaugarh fault. Importantly, the surfaces and their underlying deposits can be traced
3
4 225 continuously up to 1.5 km upstream of the Santaugarh fault along several of the major dun drainages,
5
6 226 including the Koti Nadi (Fig. 3A) and the Suarna River. In the Santaugarh fault hanging wall, deposits of the
7
8 227 proximal fan unit lie unconformably atop steeply-dipping to overturned Middle Siwalik sandstones (Thakur
9
10 228 et al., 2007) and the isolated hills unit, but our observations show that there is no evidence of offset or
11
12 229 deformation across the Santaugarh fault. Exposures along both the Koti Nadi and Suarna River indicate that
13
14 230 proximal fan sediments were deposited in steep-walled paleovalleys that were incised at least 70-75 m into
15
16 231 the underlying deposits of the isolated hills (Fig. 3B). The axes and orientations of these paleovalleys are
17
18 232 slightly offset from those of the modern river drainage system, which means that their width cannot be
19
20 233 observed directly.
21
22

234

235 Thakur et al. (2007) obtained an OSL age of 20.5 ± 1.8 ka from their unit B, and correlated this unit with an
236 age of 29.4 ± 1.7 ka from the west flank of the Suarna River valley (Singh et al., 2001), although the basis for
237 this correlation is not clear. We obtained an OSL age of 21.2 ± 1.3 ka from sample FS3.1 10 m below the fan
238 surface near the Santaugarh fault, on the east flank of the Suarna River valley (Fig. 2, Table 1).
239

240

241 The distal fan unit consists of well-bedded pebble to cobble conglomerates, with some discontinuous layers
242 of sand and silt (Singh et al., 2001; Thakur et al., 2007). The unit underlies widespread, smooth, near-planar
243 fan surfaces that occur south of, and appear to onlap against, surfaces of the proximal fan and isolated hills
244 units. These surfaces form the southern, distal expanses of the Donga and Dehradun fans, with typical
245 surface slopes (averaged over 270 m windows) of 0.2 to 1.1 degrees. Singh et al. (2001) reported OSL ages
246 of 22.8 ± 2.3 and 20.3 ± 7.5 ka from near the base of this unit, and ages of 9.4 ± 0.6 and 10.7 ± 2.4 ka near the
247 top, while Thakur et al. (2007) reported ages of 13.2 ± 1.1 and 17.1 ± 2.0 ka from the distal Donga fan.

248 Likewise, we obtained an OSL age of 14.4 ± 0.6 ka from sample FS2.2 on the west flank of the Sitla Rao, 5 m
249 below the distal fan surface (Fig. 2, Table 1). Two other samples, collected from east of the Suarna River
250 (Fig. 2), yielded OSL ages of 16.2 ± 1.4 ka (sample LIS-TOP) and 13.8 ± 0.9 ka (sample FS2.1) (Table 1). A final
251 sample (FS1.1) yielded an OSL age of 33.8 ± 3.2 ka from 3 m below the fan surface (Fig. 2, Table 1), which is

1
2 251 substantially older than any other reported age for the distal fan unit. Given its position near the southern
3
4 252 limit of the dun depositional units, and the lack of a clear textural difference between the different units, it
5
6 253 is possible that this sample was collected from an isolated distal exposure of the proximal fan unit, but at
7
8 254 present we cannot resolve this apparent discrepancy.
9

10 255

11
12 256 *Erosional volume estimates*

13
14 257 Because the original depositional surface of the isolated hills unit is not preserved, we cannot estimate the
15
16 258 volume of material that has been removed due to post-depositional incision. We therefore focus only on
17
18 259 incision of the proximal and distal fan units. Incision of the proximal fan unit on the Donga fan (Fig. 4) has
19
20 260 yielded 1900 Mm³ of sediment since abandonment of the surface, while incision on the Dehradun (Fig. 4)
21
22 261 and Bhogpur fans has yielded 750 Mm³ and 720 Mm³, respectively. In total, these add up to 3300 Mm³ of
23
24 262 sediment that has been evacuated from the dun by incision of the proximal fan unit. The distal fan unit is
25
26 263 not exposed on the Bhogpur fan, but incision of the distal unit on the Donga and Dehradun fans has yielded
27
28 264 1800 Mm³ since abandonment of the distal fan surface. Error estimates on these volumes are due largely to
29
30 265 uncertainties in mapping the fan surface remnants, and are conservatively estimated at ±20% through
31
32 266 exploration of different possible remnant configurations with various levels of certainty.
33
34 267

35
36 267

37
38 268 **Discussion**

39
40 269 *Evolution of the dun fill*

41
42 270 We interpret the sedimentary units that were deposited in the Dehra Dun since ~41 ka in terms of a
43
44 271 sequence of repeated episodes of fan deposition, backfilling, fan head incision, and basinward migration of
45
46 272 the depocenter. Such an evolutionary sequence has been widely documented for experimental fans and
47
48 273 fan deltas (Kim et al., 2006; Reitz and Jerolmack 2012; Powell et al., 2012), and may be triggered by both
49
50 274 autogenic (e.g., Kim and Muto, 2007; Kim and Jerolmack, 2008; Clarke et al., 2010; Pepin et al., 2010) and
51
52 275 allogenic (e.g., Davies and Korup, 2007; Duehnforth et al., 2008) mechanisms. In this model, the isolated
53
54 276 hills unit represents the first phase of deposition, filling accommodation that was produced by slip on the
55
56 277 Santaugarh fault and MBT and starting by at least 41 ka. The morphological expression of this unit indicates
57
58
59
60

1
2 278 that it has undergone widespread post-placement erosion, such that the original fan surface topography
3
4 279 is not preserved. It is thus impossible to use dates on the isolated hills material to identify the precise time
5
6 280 at which this depositional unit was abandoned and incised. Based on dates from the next-youngest unit,
7
8 281 however, abandonment of the isolated hills depositional regime appears to have taken place by 29-30 ka,
9
10 282 and occurred by incision of the isolated hills deposits near the sediment entry points into the basin and by a
11
12 283 major basinward shift of the active locus of deposition. This shift was followed by widespread deposition of
13
14 284 the proximal fan unit, which filled much of the available accommodation within the dun. As deposition
15
16 285 progressed, the unit began to backfill toward, and eventually across, the Santaugarh fault, eventually
17
18 286 leading to the deposition of >100 m of sediment in the hanging wall of the fault (Figs. 3B, 4).
19
20
21 287

22
23 288 Abandonment of the proximal fan deposit appears to have occurred by incision at the fan heads and a
24
25 289 second basinward shift of the depositional locus, leading to deposition of the distal fan unit. This shift took
26
27 290 place between about 23 ka (the oldest age in the distal fan unit) and 20.5 ka (the youngest age in the
28
29 291 proximal fan unit). Deposition of the distal fan unit may have eventually led to backfilling, but if so this did
30
31 292 not extend as far north as during the deposition of the proximal fan unit, and no distal fan sediments were
32
33 293 deposited in the Santaugarh fault hanging wall. The distal fan unit, in turn, was abandoned by about 10 ka,
34
35 294 when the river network entered a major phase of incision that has carved the present-day topography and
36
37 295 valley network. After 10 ka, there have been several minor episodes of aggradation and incision, leading to
38
39 296 sequences of low Holocene fill terraces along some of the major dun rivers (Nakata, 1972; Singh et al.,
40
41 297 2001). These terraces, while well-developed along the Suarna and Sitla Rao, have treads that are within 5-
42
43 298 10 m of the modern river bed levels, and are thus likely to be volumetrically insignificant in comparison
44
45 299 with the three major depositional units.
46
47
48
49 300

50 51 301 *Sediment fluxes*

52
53 302 Abandonment of the proximal fan unit led to evacuation of 3300 Mm³ of sediment, primarily via incision
54
55 303 along the major dun rivers. This evacuation must have started at 20.5-23 ka. The duration of this incision
56
57 304 episode is not known, but it must have been concluded well before the abandonment of the later distal fan
58
59
60

1
2 305 surface at 10 ka. We therefore take, as a conservative estimate, an incision duration of 13 kyr, noting that
3
4 306 the true value may be several times shorter than that. This assumption yields a time-averaged sediment
5
6 307 discharge from the proximal fan unit of $0.26 \text{ Mm}^3/\text{yr}$. This discharge must have been added to the sediment
7
8 308 loads of the Ganga and Yamuna rivers as they traversed the dun during this time period, because there is
9
10 309 only limited accommodation available for sediment storage along the river corridors within the dun.
11
12 310 Likewise, abandonment of the distal fan unit led to evacuation of 1820 Mm^3 of sediment since 10 ka,
13
14 311 directed into the Yamuna River only. This corresponds to a time-averaged sediment discharge of 0.18
15
16 312 Mm^3/yr over that time period.
17
18
19 313
20
21 314 For comparison, these time-averaged sediment discharges from the dun represent 1-2% of the summed
22
23 315 present-day suspended sediment discharge of the Ganga and Yamuna rivers, derived from 1.5% of the
24
25 316 combined Ganga and Yamuna drainage area. Dun excavation thus represents an important sediment
26
27 317 source for the Ganga and Yamuna rivers, with sediment yields comparable to the overall catchment-
28
29 318 averaged values. We stress that the time-averaged discharge values reported here almost certainly
30
31 319 underestimate the true sediment discharge from the dun, because our depositional ages provide only
32
33 320 maximum bounds on the duration of incision during abandonment of each depositional unit. For example,
34
35 321 if incision and sediment evacuation were focused in the first few thousands of years following
36
37 322 abandonment, then the 'true' time-averaged sediment discharge values could be many times higher than
38
39 323 our conservative estimates. Also, our comparison with available present-day suspended sediment discharge
40
41 324 values is made simply to provide some context for the time-averaged discharge values, and we do not know
42
43 325 either (1) the corresponding total sediment discharge, including both bedload and suspended-load
44
45 326 components, or (2) how that discharge has varied through the late Quaternary.
46
47
48
49 327
50
51 328
52
53
54
55
56
57
58
59
60

1
2 329 *Comparisons to hinterland and foreland sedimentary records*

3
4 330 The short time scale over which the major depositional units in the Dehra Dun were emplaced, and our
5
6 331 observation that there does not appear to be substantial slip on the Santaugarh fault during or after
7
8 332 deposition of the proximal fan unit, both appear to rule out major changes in fault slip rate and
9
10 333 accommodation generation as the underlying mechanism behind the abandonment of one unit and the
11
12 334 onset of deposition of the next. It seems more likely that temporal variability in sediment storage and
13
14 335 evacuation in the dun has been driven by some combination of autogenic processes and regional-scale
15
16 336 climatic variability; the latter control has been argued convincingly for the Ganga basin hinterland (e.g.,
17
18 337 Juyal et al., 2009; Ray and Srivastava, 2010) and foreland (e.g., Gibling et al., 2005; Sinha and Sarkar, 2009;
19
20 338 Roy et al., 2012). To understand the wider context of our results, we therefore compare and contrast our
21
22 339 depositional unit chronology to the timing of valley filling and incision episodes in the Ganga basin, both
23
24 340 upstream and downstream of the study area.

25
26
27
28 341

29
30 342 Upstream of the dun, Ray and Srivastava (2010) compiled a number of published studies, along with new
31
32 343 OSL dating, and argued for major phases of valley aggradation at 49-25 ka and 18-11 ka based on clustering
33
34 344 of OSL ages in terrace fill deposits. They attributed these aggradational episodes to high sediment supply
35
36 345 due to glacial-deglacial transitions. Widespread incision after 11 ka was linked by Ray and Srivastava (2010)
37
38 346 to increased monsoon precipitation after 15 ka, peaking at 9 ka, combined with post-LGM sediment
39
40 347 exhaustion. This inference was based on a number of lines of evidence for increasing monsoonal strength,
41
42 348 and thus river discharge, after 15 ka, including sedimentary (Juyal et al., 2009) and geochemical (Galy et al.,
43
44 349 2008) records. Our results from the Dehra Dun, with aggradation at ~41-33, 34-21, and 23-10 ka, agree
45
46 350 closely with this framework, indicating that the controls on sediment aggradation and incision in the
47
48 351 hinterland of the Ganga catchment also set the response of the dun. Unsurprisingly, the dun thus forms an
49
50 352 integral part of the Ganga catchment and responds near-synchronously with the hinterland, within the
51
52 353 uncertainties of the age constraints, to large-scale climatic variations. Our results also broadly agree with
53
54 354 the summary and interpretation of Pandey et al. (2014), who argued for multiple phases of alluvial
55
56 355 aggradation in the dun between >40 and 10 ka. We disagree, however, with the conclusion by Pandey et al.
57
58
59
60

1
2 356 (2014) that fan aggradation had been continuous over this period, because of the clear geometrical
3
4 357 distinction between different depositional units (Singh et al., 2001) – and we note that Pandey et al. (2014)
5
6 358 also raised the possibility of intervening erosional episodes. Thus, while the age ranges of our aggradational
7
8 359 episodes overlap in time, they represent spatially distinct aggradational events that have given rise to
9
10 360 discrete depositional units.

11
12 361

13
14 362 Downstream of the dun, Ray and Srivastava (2010) argued for two main pulses of sediment delivery to the
15
16 363 foreland: one before 26 ka (seen also by Sinha et al., 2007), and a second at 13-6 ka. The second pulse was
17
18 364 followed by incision to form the present-day Ganga channel, with the onset of incision varying from 13 to 7
19
20 365 ka at different locations between the HFT and Kanpur. More recently, Roy et al. (2012) combined new
21
22 366 stratigraphic observations in the central Ganga plains, about 300 km downstream of the HFT, with results
23
24 367 from a number of existing studies, and suggested major accumulation phases at 30-23 ka and 16-11 ka,
25
26 368 separated by episodes of incision. We compare these observations with our chronology below.

27
28
29 369

30
31
32 370 The isolated hills depositional phase that began by 41 ka in the dun coincides with lowering of the
33
34 371 floodplain in the Ganga plains (Roy et al., 2012) and declining precipitation around ~40 ka as modelled by
35
36 372 Prell and Kutzbach (1987), but there is limited, if any, evidence for aggradation within the Ganga valley.
37
38 373 Minor channel fills dated to 37 ka and levee deposits dated to 34 ka have been recorded (Roy et al., 2012),
39
40 374 but these are volumetrically small. It may be that relatively weak flow through the river systems during 41-
41
42 375 33 ka, perhaps combined with high hinterland sediment supply (Ray and Srivastava, 2010), led to
43
44 376 widespread deposition of sediment upstream of the HFT and in the dun, but was insufficient to transport
45
46 377 large sediment volumes into the plains, leading to only minor and local aggradation during this period. This
47
48 378 hypothesis would need to be tested with careful sedimentological analyses of transects extending from the
49
50 379 dun into the northern foreland. We also note that Singh et al. (2001) interpreted many of the deposits in
51
52 380 this phase as the result of debris-flow or other mass-flow processes, which would not require high water
53
54 381 discharges in the river systems.

55
56
57 382

1
2 383 The second phase of major aggradation in the dun (34-21 ka) is represented by the development of the
3
4 384 proximal fan unit, and overlaps with a period of widespread fluvial aggradation recorded downstream of
5
6 385 the dun in the Ganga plains (Goodbred, 2003; Tandon et al., 2006; Sinha and Sarkar, 2009; Ray and
7
8 386 Srivastava, 2010; Roy et al., 2012). Several of these studies have inferred the occurrence of high-intensity
9
10 387 floods in the foreland (Goodbred, 2003), while others have interpreted high sediment flux from the
11
12 388 Himalaya at this time (Taylor and Mitchell, 2000; Sharma and Owen, 1996). Given the wide extent of the
13
14 389 proximal fan unit on the floor of the dun, it is possible that the dun at this stage was essentially full, leading
15
16 390 to bypass of dun accommodation by the rivers that supply it and to high rates of sediment supply directly
17
18 391 into the foreland.
19

20
21 392

22
23 393 During the period from 28 to 16 ka, including the Last Glacial Maximum (LGM), deposition is recorded in
24
25 394 the dun by emplacement of the lower part of the distal fan unit. Aggradation in the hinterland was limited
26
27 395 during this period (Ray and Srivastava, 2010), perhaps due to limited sediment supply and glacial cover at
28
29 396 high elevations (e.g., Rahaman et al., 2009); we do not know what fraction of the distal fan unit was
30
31 397 emplaced during this time, but it may be that deposition occurred in the dun during this period because the
32
33 398 dun catchment area drains only lower-elevation Lesser Himalayan areas and was never glaciated. LGM-age
34
35 399 sediments are not found in the central Ganga plains upstream of Kanpur (Gibling et al., 2005; Sinha et al.,
36
37 400 2007); indeed, Roy et al. (2012) found no evidence for channel deposition in the Ganga valley between 25
38
39 401 and 15 ka. This hiatus has been interpreted as resulting from relatively cold, arid LGM conditions
40
41 402 (Goodbred, 2003), and it is possible that some combination of low rates of supply and low LGM river
42
43 403 discharges may have led to relatively limited sediment transport into the foreland. In the early post-glacial
44
45 404 period (16-11 ka), there is evidence for widespread deposition of the distal fan unit, perhaps driven by high
46
47 405 rates of hinterland supply (Ray and Srivastava, 2010) along with extensive slope failures and hillslope
48
49 406 sediment transport (Pratt et al., 2002). In the Ganga plains, major channel aggradation has been recorded
50
51 407 between 15.1 to 11.7 ka (Srivastava et al., 2003; Gibling et al., 2005; Tandon et al., 2006; Roy et al., 2012),
52
53 408 and has again been interpreted as being due to high rates of supply (Roy et al. 2012). We infer from this,
54
55 409 and from the wide extent of the distal fan unit, that the dun may have been filled by the later stages of
56
57
58
59
60

1
2 410 deposition of the distal fan unit and was certainly bypassed during this period, again allowing high sediment
3
4 411 discharge to the foreland.

5
6 412

7
8 413 In sum, the dun may act to modulate climate-driven variations in sediment flux from the hinterland to the
9
10 414 Ganga plains. Sediment appears to be sequestered during periods of low transport capacity and perhaps
11
12 415 when the dun is underfilled, but dun aggradation is somewhat independent of hinterland sediment supply.

13
14 416 In contrast, sediment is exported during periods of high transport capacity and incision of the dun fill, and

15
16 417 also during periods of high hinterland supply when the dun is filled and bypassed. Several of the times of

17
18 418 widespread aggradation within the dun (~41-33 ka, 23-16 ka) coincide with periods of limited downstream

19
20 419 deposition, and we infer that during these periods the dun may have acted as a partial, transient sediment

21
22 420 trap, perhaps due to some combination of low river discharges or low rates of hinterland supply. Later,

23
24 421 however, due to some combination of rising discharge and increasing hinterland supply, we infer that the

25
26 422 dun 'filled and spilled', in concert with widespread downstream aggradation at 34-21 ka and 15-12 ka.

27
28 423

29
30
31
32 424 *Comparison to the Gandak River*

33
34 425 Our results from the Dehra Dun help to place constraints on the timing and magnitude of its contribution to

35
36 426 sediment flux in the Ganga and Yamuna rivers. To what extent is this model applicable to other duns along

37
38 427 the Himalayan front? To answer this question, we compare our results with observations from several

39
40 428 other large Himalayan river systems, the Gandak and Kosi rivers. The Gandak River (also referred to as the

41
42 429 Narayani River in southern Nepal) flows through the Chitwan Dun (Fig. 1), which has developed between

43
44 430 strands of the MBT and Main Dun Thrust to the north and the HFT system to the south (Fig. 5). As in the

45
46 431 Dehra Dun, the Chitwan Dun is impounded behind anticlinal ridges of Siwalik sediments developed above

47
48 432 strands of the HFT (Lavé and Avouac, 2000, 2001). Estimates of the present-day suspended sediment

49
50 433 discharge of the Gandak near Narayangarh, at the upstream entrance to the Chitwan Dun, are 105-110

51
52 434 Mt/yr (Lavé and Avouac, 2001; Garzanti et al., 2007), while Lupker et al. (2012) used cosmogenic

53
54 435 radionuclides to estimate total sediment discharge of 110-184 Mt/yr. At Tribeni, near the downstream end

55
56 436 of the dun, Sinha and Friend (1994) estimated a suspended sediment discharge of 79 Mt/yr. These values

57
58
59
60

1
2 437 are equivalent to volumetric discharges of $\sim 30\text{-}70 \text{ Mm}^3/\text{yr}$. Note that the much larger sediment discharge
3
4 438 estimates of $450\text{-}510 \text{ Mt/yr}$ by Singh et al. (2008) are based on a mixing model, and may not be directly
5
6 439 comparable. At present, the river occupies a wide, low-gradient meander belt across the Chitwan Dun and
7
8 440 is not substantially incised into the dun floor, perhaps indicating that accommodation in the dun is nearly
9
10 441 full.

11
12 442

13
14 443 Within the Chitwan Dun, sediment from the Gandak and Rapti Rivers, and from smaller basins that drain
15
16 444 the Main Dun Thrust hangingwall, has been deposited in a series of interfingering fans and fill terraces (Fig.
17
18 445 5), which form extensive low-gradient depositional surfaces similar to those of the Dehra Dun (Kimura,
19
20 446 1995, 1999). Kimura (1995) identified three main depositional units that could be correlated across multiple
21
22 447 catchment-fan systems. While interpretation of his assignments is somewhat complicated by uncertainty in
23
24 448 correlation between different lithostratigraphic units, the two youngest units broadly comprise (1) an older
25
26 449 set of fan remnants (the Barakot and Belani deposits) with quasi-planar to slightly convex-up surfaces that
27
28 450 range from ~ 180 to 300 m above the modern river beds, (2) a more extensive, younger set of planar fan
29
30 451 remnants (the Bishannagar and Kirtipur deposits) that are clearly inset into, and onlap, the older remnants,
31
32 452 and form widespread near-planar surfaces, $10\text{-}70 \text{ m}$ above the modern river beds (Fig. 5).

33
34 453

35
36
37
38 454 No absolute ages are available for the Chitwan Dun fill deposits, although Kimura (1995) suggested ages of
39
40 455 $26\text{-}16 \text{ ka}$ and $<10 \text{ ka}$ for the two youngest depositional units. On the basis of surface morphology, deposit
41
42 456 geometry, and cross-cutting relationships between units, we tentatively correlate the older fan remnants
43
44 457 (Barakot and Belani deposits) with the proximal fan unit in the Dehra Dun, and the younger fan remnants
45
46 458 (Bishannagar and Kirtipur deposits) with the Dehra Dun distal fan unit. This does not, of course, imply that
47
48 459 the depositional ages are similar in these two settings, only that the deposits occupy similar spatial settings
49
50 460 and have similar geometrical relationships. This correlation must be tested with more careful mapping and
51
52 461 dating of the Chitwan Dun fill.

53
54 462
55
56
57
58
59
60

1
2 463 If we accept the correlations of Kimura (1995) and apply the same techniques to determine incision depths
3
4 464 and erosional volumes as we used in the Dehra Dun, then we find that incision of the older fan remnants
5
6 465 has removed a volume of 6300 Mm³, while incision of the younger fan remnants has removed 2400 Mm³
7
8 466 from the dun (Fig. 5). If we further assume that incision of the younger fan remnants began at around 10
9
10 467 ka, as with the correlative deposits in the Dehra Dun, then this evacuation would imply a time-averaged
11
12 468 sediment discharge of ~0.2 Mm³/yr, about 1% of the modern Gandak suspended sediment discharge. We
13
14 469 stress, however, that the timing of deposition and incision in the Chitwan Dun remains unconstrained, and
15
16 470 so such estimates must remain indicative.

17
18
19 471

20
21 472 Downstream of the HFT, the Gandak has built a highly avulsive fan system in the foreland (Gupta, 1997).
22
23 473 Sinha et al. (2014a) used resistivity surveys and limited borehole data to document two lithological units
24
25 474 within the upper 100 m of the fan: a lower unit characterized by narrow but thick (>40 m) channel fills set
26
27 475 into thick muds, and an upper unit that comprises thinner, laterally-stacked sand bodies separated by mud
28
29 476 layers. Importantly, channel fills are discontinuous in both units, perhaps due to depositional hiatuses
30
31 477 caused by episodic trapping of sediment in the dun (Sinha et al., 2014a). The observation that the dun
32
33 478 appears to be nearly full at the present day may explain the high modern sediment discharge of the Gandak
34
35 479 (e.g., Singh et al., 2008), and may be analogous to the bypass conditions inferred for the Dehra Dun at 34-
36
37 480 21 or 16-11 ka.

38
39
40
41 481

42 482 *Comparison to the Kosi River*

43
44
45 483 In contrast to the Yamuna, Ganga, and Gandak, the Kosi River debouches directly into the Ganga plain in
46
47 484 eastern Nepal (Fig. 1, Fig. 6). Late Quaternary deformation appears to be focused on the HFT system at the
48
49 485 mountain front (Lave and Avouac, 2001), and the lack of propagation into the foreland has resulted in an
50
51 486 abrupt mountain front and a relatively short distance (as little as 5-8 km) between the HFT and MBT
52
53 487 systems (Schelling, 1992; Lave and Avouac, 2001). The thrust sheet between the HFT and MBT is composed
54
55 488 of relatively weak Middle and Lower Siwalik foreland basin rocks in the HFT hangingwall (Fig. 6), with local
56
57 489 relief (measured over a 1 km radius to reflect typical hillslope lengths) of up to 1 km. Estimates of the
58
59
60

1
2 490 present-day suspended sediment discharge of the Kosi range from 95 Mt/yr and 43 Mt/yr at Barakhshetra
3
4 491 and Baltara, respectively (Sinha and Friend, 1994; Sinha et al., 2005) to 175 Mt/yr (Lave and Avouac, 2001),
5
6 492 while Gohain and Parkash (1990) reported a much higher value of 345 Mt/yr. Lupker et al. (2012) used
7
8 493 cosmogenic radionuclides to estimate a longer-term total sediment discharge of 69-141 Mt/yr. Apart from
9
10 494 the high estimate of Gohain and Parkash (1990), these values are equivalent to volumetric discharges of
11
12 495 ~30-70 Mm³/yr, broadly comparable to those of the Gandak (although derived from approximately twice
13
14 496 the drainage area).

15
16
17 497

18
19 498 Downstream of the HFT, the Kosi River has constructed a large, highly avulsive fan system (Chakraborty et
20
21 499 al., 2010; Sinha et al., 2013), with evidence for rapid historical aggradation (Desai, 1982; Sinha et al.,
22
23 500 2014b). Subsurface investigation of the top ~100 m by Sinha et al. (2014a) reveals widespread multi-story
24
25 501 sand bodies, 20-30 m thick, with thick gravel deposits in the proximal fan. Sinha et al. (2014a) interpreted
26
27 502 this depositional architecture, along with the short avulsion timescale of the Kosi River (approx. 24 years),
28
29 503 as being due to the lack of intermediate sediment storage upstream of the fan. This contrasts with the
30
31 504 Gandak River, which, despite comparable present-day (Sinha et al., 2005) and late Holocene (Lupker et al.,
32
33 505 2012) sediment discharge and a higher suspended sediment yield, has built a fan with finer overall grain
34
35 506 sizes and much more isolated channel bodies within the subsurface (Sinha et al., 2014a). These
36
37 507 observations agree with our interpretation from the Dehra Dun and Chitwan Dun that proximal dun storage
38
39 508 can 'filter' hinterland sediment supply, amplifying high discharge values but also acting as a transient
40
41 509 sediment store during periods of low sediment discharge to the foreland.
42
43
44

45 510

46 47 511 *Conceptual model*

48
49 512 We summarise our results from all river systems in a conceptual model of temporal variations in sediment
50
51 513 supply to the foreland in both the presence, and absence, of a dun (Fig. 7). Our key inference from the field
52
53 514 observations is that intermediate dun sediment storage and release will act to modulate and amplify the
54
55 515 sediment supply to the foreland. This may occur through changes in hinterland sediment supply, changes in
56
57 516 transport capacity, or both. Sediment is sequestered in the dun during periods of low transport capacity
58
59
60

1
2 517 and either high or low hinterland supply, leading to underfilled conditions (Fig. 7A). Sediment is evacuated
3
4 518 from the dun when either (1) transport capacity is high, resulting in incision of the dun fill, or (2) both
5
6 519 hinterland supply and transport capacity are high, leading to filling of the dun and spilling of sediment into
7
8 520 the foreland (Fig. 7B). In contrast, rivers without proximal storage are likely to be characterised by a more
9
10 521 continuous, less temporally-variable sediment flux (Fig. 7C), leading perhaps to enhanced likelihood of
11
12 522 'stacking' of channel units in the foreland. Rivers without duns may also be more prone to bed aggradation
13
14 523 and subsequent avulsion, as in the modern Kosi River (Sinha, 2009; Chakraborty et al., 2010), although it is
15
16 524 important to note that avulsion frequency is dependent on a number of other variables as well (e.g., Bryant
17
18 525 et al., 1995; Mohrig et al., 2000; Wickert et al., 2013; Sinha et al., 2014b). It is also important to recall that
19
20 526 large-scale behaviour and evolution of the major Himalayan river systems depends on a range of factors
21
22 527 (e.g., Sinha et al., 2005), of which transient storage in a dun is but one example. Unravelling the relative
23
24 528 importance of these factors will require enhanced understanding of sediment fluxes over different time
25
26 529 scales, and careful study of the links between proximal and distal sediment stores along these rivers.
27
28
29

30 530

31
32 531 This model highlights the importance of understanding the tectonic 'template', or spatial distribution and
33
34 532 rates of rock uplift. This template is critical, not just because it helps to set erosion rates in the hinterland of
35
36 533 the major river systems (e.g., Sinha et al., 2005; Scherler et al., 2014), but because the distribution of rock
37
38 534 uplift at the mountain front dictates whether or not piggyback basins or other local depocentres are likely
39
40 535 to form at the mountain front. Distributed tectonic activity also implies more spatially-distributed foreland
41
42 536 subsidence, such that the rate of accommodation generation immediately adjacent to the mountain front is
43
44 537 likely to be lower in the presence of a dun bounded by multiple active faults. While there has been some
45
46 538 effort to understand Holocene rates of slip on structures associated with the HFT (e.g., Wesnousky et al.,
47
48 539 1999; Kumar et al., 2006; Sapkota et al., 2013), our results point to the need for better assessment of the
49
50 540 full pattern of rock uplift along faults bounding the Himalayan duns.
51
52

53 541

54
55
56 542 We have inferred the link between upstream sediment supply and downstream fluvial response using
57
58 543 available stratigraphic and age data from the Ganga Basin. It would be useful to explore the possible
59
60

1
2 544 implications of episodic storage and release for spatial variations in specific sediment characteristics. For
3
4 545 example, Granet et al. (2007, 2010) used U-Th disequilibria to estimate transfer times of both suspended
5
6 546 and bedload sediment in the Ganga and Gandak rivers. A natural question is whether river systems without
7
8 547 a dun, such as the Kosi or Karnali, show evidence for more rapid transfer than those systems with abundant
9
10 548 upstream storage. A more systematic study of these variations could help improve our large-scale
11
12 549 understanding of sediment movement through the entire Ganga sediment routing system (e.g., Bloethe
13
14 550 and Korup, 2013).

15 551

16 552 **Conclusions**

17
18
19 553 We investigate the timing and magnitude of sediment storage and evacuation from the Dehra Dun, a
20
21 554 piggyback basin in northwestern India, in order to understand the effects of this time-varying sediment
22
23 555 source on the downstream morphology of the major river systems that drain through the dun. The dun
24
25 556 shows evidence for at least three phases of late Quaternary sedimentation, at ~41-33, 34-21, and 23-10 ka.
26
27 557 During each of these phases, sediment fans built out into the dun, accompanied in at least the later stages
28
29 558 by fill terrace deposition along the Ganga and Yamuna rivers. Each progradation phase was followed by fan-
30
31 559 head incision, abandonment of the active depositional lobes, and a basinward shift of the depocentre. The
32
33 560 volumes of sediment released during these incision phases, when divided by the maximum time span
34
35 561 available for incision, yield estimates of palaeo-sediment discharge that are 1-2% of the modern
36
37 562 suspended-sediment loads of the Ganga and Yamuna rivers, from about 1.5% of the combined catchment
38
39 563 areas of these rivers. Our results show that the dun fill is highly dynamic, with major changes in both
40
41 564 volume and depocentre location on $\sim 10^4$ yr time scales.

42 565

43
44
45 566 The early stages of at least two episodes of sediment storage in the dun appear to coincide with periods of
46
47 567 upstream aggradation in the hinterland and partial depositional hiatuses in the Ganga plains, indicating that
48
49 568 the dun may act as a partial, transient sediment trap. Later phases of dun aggradation, and subsequent
50
51 569 excavation and evacuation of dun sediment, correspond to periods of widespread downstream
52
53 570 aggradation. The dun may thus amplify climate-induced variations in sediment supply to the major river
54
55
56
57
58
59
60

1
2 571 systems. This model appears to explain some contrasting features of the Gandak and Kosi river systems in
3
4 572 central Nepal; the presence of a dun along the Gandak has led to episodic storage and release of sediment
5
6 573 upstream of the Himalayan mountain front and construction of a mud-rich fan in the Ganga plains. In
7
8 574 contrast, the Kosi River debouches directly into the foreland, and the lack of upstream storage means that a
9
10 575 more continuous supply of sediment has built a coarse-grained, highly avulsive fan characterised by stacked
11
12 576 multi-story channel bodies. We infer from these examples that the tectonic framework at the mountain
13
14 577 front – specifically, the way in which shortening is distributed across different faults – plays a critical role in
15
16 578 determining downstream river morphology, stratigraphy, and evolution.
17
18
19 579

20 21 580 **Acknowledgements**

22
23 581 This work was supported by a grant from the UK-India Education and Research Initiative (SA-07-06F).
24
25 582 Sanjeev Gupta has provided very helpful guidance and ideas throughout the project. We thank Jason
26
27 583 Barnes, Elizabeth Dingle, and Jack Pickering for useful discussions and assistance in the field, and the
28
29 584 participants of the Royal Society/DST International Seminar on River Dynamics in the Ganga Plains for their
30
31 585 perspectives and input. We also thank N. Suresh at the Wadia Institute of Himalayan Geology for assistance
32
33 586 with the OSL dating. Comments by journal editor Peter van der Beek, and constructive reviews by Mikael
34
35 587 Attal and two anonymous reviewers, helped to improve the manuscript.
36
37
38 588

39 40 41 589 **References**

- 42
43 590 ABBAS, N., & SUBRAMANIAN, V. (1984) Erosion and sediment transport in the Ganges River basin (India). *J.*
44
45 591 *Hydrology*, 69, 173-182.
46
47 592 ALLEN, P.A., & DENSMORE, A. L. (2000) Sediment flux from an uplifting fault block. *Basin Research*, 12, 367-
48
49 593 380.
50
51 594 BARNES, J.B., DENSMORE, A.L., MUKUL, M., SINHA, R., JAIN, V., & TANDON, S.K. (2011) Interplay between
52
53 595 faulting and base level in the development of Himalayan frontal fold topography. *Journal of*
54
55 596 *Geophysical Research – Earth Surface*, 116, F03012, doi:10.1029/2010JF001841.
56
57
58 597 BLOETHE, J. & KORUP, O. (2013) Millennial lag times in the Himalayan sediment routing system. *Earth and*
59
60

- 1
2 598 *Planetary Science Letters*, 382, 38-46.
- 3
4 599 BLUM, M.D., & TÖRNQVIST, T.E. (2000) Fluvial responses to climate and sea-level change: a review and look
5
6 600 forward. *Sedimentology*, 47, 2-48.
- 7
8 601 BRYANT, M., FALK, P., & PAOLA, C. (1995) Experimental study of avulsion frequency and rate of deposition.
9
10 602 *Geology*, 23, 365-368.
- 11
12 603 CARRETIER, S., & LUCAZEAU, F. (2005) How does alluvial sedimentation at range fronts modify the erosional
13
14 604 dynamics of mountain catchments? *Basin Research*, 17, 341-361.
- 15
16 605 CASTELLTORT, S., & VAN DEN DRIESSCHE, J. (2003) How plausible are high-frequency sediment supply-
17
18 606 driven cycles in the stratigraphic record? *Sedimentary Geology*, 157, 3-13.
- 19
20 607 CHAKRABORTY, T., KAR, R., GHOSH, P., & BASU, S., 2010. Kosi megafan: Historical records, geo- morphology
21
22 608 and the recent avulsion of the Kosi River. *Quaternary International*, 227, 143–160.
- 23
24 609 CHAKRAPANI, G.J., & SAINI, R. K. (2009) Temporal and spatial variations in water discharge and sediment
25
26 610 load in the Alaknanda and Bhagirathi Rivers in Himalaya, India. *Journal of Asian Earth Sciences*, 35, 545-
27
28 611 553.
- 29
30 612 CLARKE, L., QUINE, T.A., & NICHOLAS, A.P. (2010) An experimental investigation of autogenic behavior
31
32 613 during alluvial fan evolution. *Geomorphology*, 115, 278-285.
- 33
34 614 CLIFT, P. (2006) Controls on the erosion of Cenozoic Asia and the flux of clastic sediment to the ocean. *Earth*
35
36 615 *and Planetary Science Letters*, 241, 571-580
- 37
38 616 DAVIES, T., & KORUP, O. (2007) Persistent alluvial fanhead trenching resulting from large, infrequent
39
40 617 sediment inputs. *Earth Surface Processes and Landforms*, 32, 725-742.
- 41
42 618 DECELLES, P.G., & GILES, K.A. (1996) Foreland basin systems. *Basin Research*, 8, 105-123.
- 43
44 619 DECELLES, P.G., & HORTON, B.K. (2003) Early to middle Tertiary foreland basin development and the history
45
46 620 of Andean crustal shortening in Bolivia. *Geological Society of America Bulletin*, 115, 58–77.
- 47
48 621 DECELLES, P.G., GRAY, M.B., RIDGWAY, K.D., COLE, R.B., PIVNIK, D.A., PEQUERA, N. & SRIVASTAVA, P.
49
50 622 (1991) Controls on synorogenic alluvial-fan architecture, Beartooth Conglomerate (Palaeocene),
51
52 623 Wyoming and Montana. *Sedimentology*, 38, 567-590.
- 53
54 624 DUEHNFORH, M., DENSMORE, A.L., IVY-OCHS, S., & ALLEN, P.A. (2008) Controls on sediment evacuation
55
56
57
58
59
60

- 1
2 625 from glacially modified and unmodified catchments in the eastern Sierra Nevada, California. *Earth*
3
4 626 *Surface Processes and Landforms*, 33, 1602-1613.
- 5
6 627 DUTTA, S., SURESH, N. & KUMAR, R. (2012). Climatically controlled Late Quaternary terrace staircase
7
8 628 development in the fold- and thrust belt of the Sub Himalaya. *Palaeogeography, Palaeoclimatology,*
9
10 629 *Palaeoecology*, 356–357, 16-26.
- 11
12 630 GALY, A., & FRANCE-LANORD, C. (2001) Higher erosion rates in the Himalaya: geochemical constraints on
13
14 631 riverine fluxes. *Geology*, 29, 23–26.
- 15
16 632 GALY, V., FRANCOIS, L., FRANCE-LANORD, C., FAURE, P., KUDRASS, H., PALHOL, F., & SINGH, S.K. (2008) C4
17
18 633 plants decline in the Himalayan basin since the Last Glacial Maximum. *Quaternary Science Reviews*, 27,
19
20 634 1396-1409.
- 21
22 635 GARZANTI, E., VEZZOLI, G., ANDO, S., LAVE, J., ATTAL, M., FRANCE-LANORD, C., & DECELLES, P. (2007)
23
24 636 Quantifying sand provenance and erosion (Marsyandi River, Nepal Himalaya). *Earth and Planetary*
25
26 637 *Science Letters*, 258, 500-515.
- 27
28 638 GIBLING, M.R. TANDON, S.K., SINHA, R. & JAIN, M. (2005) Discontinuity-bounded alluvial sequences of the
29
30 639 southern Gangetic plains, India: aggradation and degradation in response to monsoonal strength.
31
32 640 *Journal of Sedimentary Research*, 75, 373-389.
- 33
34 641 GIBLING, M.R., FIELDING, C.R., & SINHA, R. (2011) Alluvial valleys and alluvial sequences: towards a
35
36 642 geomorphic assessment, *SEPM Special Publication*, 97, 423–447.
- 37
38 643 GOHAIN, K., & PARKASH, B. (1990) Morphology of the Kosi Megafan. In: *Alluvial Fans: A Field Approach* (Ed.
39
40 644 by A.H. Rackchoki and M. Church), pp. 151-178. John Wiley and Sons Ltd.
- 41
42 645 GOODBRED, S. (2003) Response of the Ganges dispersal system to climate change: a source-to-sink view
43
44 646 since the last interstade. *Sedimentary Geology*, 162, 83-104.
- 45
46 647 GRANET, M., CHABAUX, F., FRANCE-LANORD, C., STILLE, P., & PELT, E. (2007) Time-scales of sedimentary
47
48 648 transfer and weathering processes from U-series nuclides: clues from the Himalayan rivers. *Earth and*
49
50 649 *Planetary Science Letters*, 261, 389-406.
- 51
52
53
54
55
56
57
58
59
60

- 1
2 650 GRANET, M., CHABAUX, F., STILLE, P., DOSSETO, A., FRANCE-LANORD, C., & BLAES, E. (2010) U-series
3
4 651 disequilibria in suspended river sediments and implication for sediment transfer time in alluvial plains:
5
6 652 the case of the Himalayan rivers. *Geochimica et Cosmochimica Acta*, 74, 2851-2865.
7
8 653 GUPTA, S. (1997) Himalayan drainage patterns and the origin of fluvial megafans in the Ganges foreland
9
10 654 basin. *Geology*, 25, 11–14,
11
12 655 HILLEY, G.E., & STRECKER, M.R. (2005) Processes of oscillatory basin filling and excavation in a tectonically
13
14 656 active orogen: Quebrada del Toro Basin, NW Argentina. *Geological Society of America Bulletin*, 117,
15
16 657 887-901.
17
18 658 JHA, P.K., SUBRAMANIAN, V., & SITASAWAD, R. (1988) Chemical and sediment mass transfer in the Yamuna
19
20 659 river- a tributary of the Ganges system. *Journal of Hydrology*, 104, 237-246.
21
22 660 JUYAL, N., PANT, R.K., BASAVAIHAH, N., BHUSHAN, R., JAIN, M. SAINI, N.K., YADAVA, M.G., & SINGHVI, A.K.
23
24 661 (2009) Reconstruction of Last Glacial to early Holocene monsoon variability from relict lake sediment
25
26 662 of the Higher Central Himalaya, Uttarakhand, India. *Journal of Asian Earth Sciences*, 34, 437-449.
27
28 663 KIM, W., & MUTO, T. (2007) Autogenic response of alluvial-bedrock transition to base level variation:
29
30 664 experiment and theory. *Journal of Geophysical Research – Earth Surface*, 112, F03S14,
31
32 665 doi:10.1029/2006JF000561.
33
34 666 KIM, W., & JEROLMACK, D.J. (2008) The pulse of calm fan deltas. *Journal of Geology*, 116, 315-330.
35
36 667 KIM, W., PAOLA, C., SWENSON, J.B., & VOLLER, V.R. (2006) Shoreline response to autogenic processes of
37
38 668 sediment storage and release in the fluvial system. *Journal of Geophysical Research – Earth Surface*,
39
40 669 111, F04013, doi:10.1029/2006JF000470.
41
42 670 KIMURA, K. (1995) Terraced debris and alluvium as indicators of the Quaternary structural development of
43
44 671 the northwestern Chitwan Dun, central Nepal. *The Science Reports of the Tohoku University, 7th Series*
45
46 672 (*Geography*), 45, 103-120.
47
48 673 KIMURA, K. (1999) Diachronous evolution of sub-Himalayan piggyback basins, Nepal. *The Island Arc*, 8, 99-
49
50 674 113.
51
52
53
54
55
56
57
58
59
60

- 1
2 675 KUMAR, S., WESNOUSKY, S.G., ROCKWELL, T.K., BRIGGS, R.W., THAKUR, V.C., & JAYANGONDAPERUMAL, R.
3
4 676 (2006) Paleoseismic evidence of great surface rupture earthquakes along the Indian Himalaya. *Journal*
5
6 677 *of Geophysical Research – Solid Earth*, 111, B03304, doi:10.1029/2004JB003309.
7
8 678 LANCASTER, S.T., & CASEBEER, N.E. (2007) Sediment storage and evacuation in headwater valleys at the
9
10 679 transition between debris-flow and fluvial processes. *Geology*, 35, 1027-1030.
11
12 680 LANE, S.N., & RICHARDS, K.S. (1997) Linking river channel form and process: time, space, and causality
13
14 681 revisited. *Earth Surface Processes and Landforms*, 22, 249-260.
15
16 682 LAVÉ, J., & AVOUAC, J.P. (2000) Active folding of fluvial terraces across the Siwaliks Hills, Himalayas of
17
18 683 central Nepal. *Journal of Geophysical Research – Solid Earth*, 105, 5735-5770.
19
20 684 LAVÉ, J., & AVOUAC, J.P. (2001) Fluvial incision and tectonic uplift across the Himalayas of central Nepal.
21
22 685 *Journal of Geophysical Research – Solid Earth*, 106, 26561-26591.
23
24 686 LETURMY, P., MUGNIER, J.L., VINOUR, P., BABY, P., COLLETTA, B., & CHABRON, E. (2000) Piggyback basin
25
26 687 development above a thin-skinned thrust belt with two detachment levels as a function of interactions
27
28 688 between tectonic and superficial mass transfer: The case of the Subandean Zone (Bolivia).
29
30 689 *Tectonophysics*, 320, 45-67.
31
32 690 LUPKER, M., FRANCE-LANORD, C., GALY, V., LAVÉ, J., GAILLARDET, J., GAJUREL, A.P., GUILMETTE, C.,
33
34 691 RAHMAN, M., SINGH, S.K., & SINHA, R. (2012) Predominant floodplain over mountain weathering of
35
36 692 Himalayan sediments (Ganga basin). *Geochemica Cosmochemica Acta*, 84, 410-432.
37
38 693 MALMON, D.V., RENEAU, S.L., DUNNE, T., KATZMAN, D. & DRAKOS, P.G. (2005) Influence of sediment
39
40 694 storage on downstream delivery of contaminated sediment. *Water Resources Research*, 41, W05008,
41
42 695 doi:10.1029/2004WR003288.
43
44 696 MEADE, R.H. (1982) Sources, sinks and storage of river sediment in the Atlantic drainage of the United
45
46 697 States. *Journal of Geology*, 90, 235-252.
47
48 698 MOHRIG, D., HELLER, P.L., PAOLA, C., & LYONS, W.J. (2000) Interpreting avulsion process from ancient
49
50 699 alluvial sequences; Guadalope-Matarranya system (northern Spain) and Wasatch Formation (western
51
52 700 Colorado). *Geological Society of America Bulletin*, 112, 1787-1803, doi:10.1130/0016-
53
54 701 7606(2000)112<1787:IAPFAA>2.0.CO;2.
55
56
57
58
59
60

- 1
2 702 MUGNIER, J.L., LETURMY, P., MASCLE, G., HUYGHE, P., CHALARON, E., VIDAL, G., HUSSON, L. & DELCAILLAU,
3
4 703 B. (1999a). The Siwaliks of western Nepal: I. Geometry and kinematics. *Journal of Asian Earth Sciences*,
5
6 704 17, 629-642.
- 7
8 705 MUGNIER, J.L., LETURMY, P., HUYGHE, P., & CHALARON, E. (1999b) The Siwaliks of western Nepal II:
9
10 706 Mechanics of the thrust wedge. *Journal of Asian Earth Sciences*, 17, 643-657.
- 11
12 707 MUKHOPADHYAY, D. K., & MISHRA, P. (2004) The Main Frontal Thrust (MFT), northwestern Himalayas:
13
14 708 Thrust trajectory and hanging wall fold geometry from balanced cross sections. *Journal of the*
15
16 709 *Geological Society of India*, 64, 739-746.
- 17
18 710 NAKATA T. (1972) Geomorphologic history and crustal movements of the foothills of the Himalayas. *Science*
19
20 711 *Reports, Tohoku University*, 22, 39-177.
- 21
22 712 NAKATA, T. (1989) Active faults of the Himalaya of India and Nepal. In: *Tectonics of the Western Himalayas*
23
24 713 (Ed. by L. L. Malinconico and R. J. Lillie), *Spec. Pap. Geol. Soc. Am.*, 232, pp. 243-264.
- 25
26 714 NOSSIN, J.J. (1971) Outline of the geomorphology of the Doon valley, northern U.P., India. *Zeitschrift*
27
28 715 *Geomorphology N.F.*, 12, 18-50.
- 29
30 716 ORI, G.G., & FRIEND, P.F. (1984) Sedimentary basins formed and carried piggyback on active thrust sheets.
31
32 717 *Geology*, 12, 475-478.
- 33
34 718 OVERPECK, J., ANDERSON, D., TRUMBORE, S., & PRELL, W. (1996) The southwest Indian monsoon over the
35
36 719 last 18000 years. *Climate Dynamics*, 12, 213–225.
- 37
38 720 PANDEY, A.K., PANDEY, P., SINGH, G.D., & JUYAL, N. (2014) Climate footprints in the Late Quaternary-
39
40 721 Holocene landforms of Dun Valley, NW Himalaya, India. *Current Science*, 106, 245-253.
- 41
42 722 PAOLA, C. (2000) Quantitative models of sedimentary basin filling. *Sedimentology*, 47, 121-178.
- 43
44 723 PEPIN, E., CARRETIER, S., & HERAIL, G. (2010) Erosion dynamics modelling in a coupled catchment-fan
45
46 724 system with constant external forcing. *Geomorphology*, 122, 78-90.
- 47
48 725 PHILLIPS, J.D. (1991) Fluvial sediment budgets in the North Carolina Piedmont. *Geomorphology*, 4, 231-241.
- 49
50 726 POWELL, E. J., W. KIM, & T. MUTO (2012) Varying discharge controls on timescales of autogenic storage and
51
52 727 release processes in fluvio-deltaic Environments: Tank Experiments. *Journal of Geophysical Research –*
53
54 728 *Earth Surface*, 117, F02011, doi:10.1029/2011JF002097.
- 55
56
57
58
59
60

- 1
2 729 POWERS, P.M., LILLIE, R.J., & YEATS, R.S. (1998) Structure and shortening of the Kangra and Dehra Dun
3
4 730 reentrants, Sub-Himalaya, India. *Geological Society of America Bulletin*, 110, 1010-1027.
5
6 731 PRATT, B., BURBANK, D.W., HEIMSATH, A., & OJHA, T. (2002) Impulsive alluviation during early Holocene
7
8 732 strengthened monsoons, central Nepal Himalaya. *Geology* 30, 911-914.
9
10 733 PRELL, W.L., & KUTZBACH, J.E. (1987) Monsoon variability over the past 150,000 years. *Journal of*
11
12 734 *Geophysical Research – Solid Earth*, 92, 8411-8425.
13
14 735 RAHAMAN, W., SINGH, S.K., SINHA, R., & TANDON, S.K. (2009) Climate control on erosion distribution over
15
16 736 the Himalaya during the past ~100 ka. *Geology*, 37, 559-562.
17
18 737 RAIVERMAN, V. (1997), On dating of the Himalayan Thrusts. *Himalayan Geology*, 18, 63-79.
19
20 738 RAIVERMAN, V., SRIVASTAVA, A.K., & PRASAD, D.N. (1993) On the foothill thrust of the Northwestern
21
22 739 Himalaya. *J. Himalayan Geology*, 4, 237-256.
23
24 740 RAY, Y., & SRIVASTAVA, P. (2010) Widespread aggradation in the mountainous catchment of the
25
26 741 Alaknanda-Ganga River System: timescales and implications to hinterland-foreland relationships.
27
28 742 *Quaternary Science Reviews*, 29, 2238-2260.
29
30 743 REITZ, M.D., & JEROLMACK, D.J. (2012) Experimental alluvial fan evolution: Channel dynamics, slope
31
32 744 controls, and shoreline growth. *Journal of Geophysical Research – Earth Surface*, 117, F02021,
33
34 745 doi:10.1029/2011JF002261.
35
36 746 ROY, N.G., SINHA, R., & GIBLING, M.R. (2012) Aggradation, incision, and interfluvial flooding in the Ganga
37
38 747 Valley over the past 100,000 years: testing the influence of monsoonal precipitation.
39
40 748 *Palaeogeography, Palaeoclimatology, Palaeoecology*, 356-357, 38-53.
41
42 749 SAPKOTA, S.N., BOLLINGER, L., KLINGER, Y., TAPPONNIER, P., GAUDEMER, Y., & TIWARI, D. (2012) Primary
43
44 750 surface ruptures of the great Himalayan earthquakes in 1934 and 1255. *Nature Geoscience*, 6, 71-76.
45
46 751 SCHELLING, D. (1992) The tectonostratigraphy and structure of the eastern Nepal Himalaya. *Tectonics*, 11,
47
48 752 925-943.
49
50 753 SCHERLER, D., BOOKHAGEN, B., & STRECKER, M.R. (2014) Tectonic control on ¹⁰Be-derived erosion rates in
51
52 754 the Garhwal Himalaya, India. *Journal of Geophysical Research – Earth Surface*, 119,
53
54 755 doi:10.1029/2013JF002955.
55
56
57
58
59
60

- 1
2 756 SHARMA, M.C., & OWEN, L.A. (1996) Quaternary glacial history of the Garhwal Himalaya, India. *Quaternary*
3
4 757 *Science Reviews*, 15, 335-365.
- 5
6 758 SIMPSON, G. (2010) Influence of the mechanical behaviour of brittle-ductile fold-thrust belts on the
7
8 759 development of foreland basins. *Basin Research*, 22, 139-156.
- 9
10 760 SINGH, A.K., PARKASH, B., MOHINDRA, A., THOMAS, J.V., & SINGHVI, A.K. (2001) Quaternary alluvial fan
11
12 761 sedimentation in the Dehradun Valley Piggyback Basin, NW Himalaya: tectonic and palaeoclimatic
13
14 762 implications. *Basin Research*, 13, 449-471.
- 15
16
17 763 SINGH, S.K., RAI, S.K., & KRISHNASWAMI, S. (2008) Sr and Nd isotopes in river sediments from the Ganga
18
19 764 Basin: sediment provenance and spatial variability in physical erosion. *J. Geophys. Res.*, 113, F03006,
20
21 765 doi:10.1029/2007JF000909.
- 22
23 766 SINHA, R. (2009) The Great avulsion of Kosi on 18 August 2008. *Current Science*, 97, 429-433.
- 24
25 767 SINHA, R., & FRIEND, P.F. (1994) River systems and their sediment flux, Indo-Gangetic plains, Northern
26
27 768 Bihar, India. *Sedimentology*, 41, 825-845.
- 28
29
30 769 SINHA, R., & SARKAR, S. (2009) Climate-induced variability in the Late Pleistocene-Holocene fluvial and
31
32 770 fluvio-deltaic successions in the Ganga plains, India. *Geomorphology*, 113, 173-188.
- 33
34 771 SINHA, R., JAIN, V., PRASAD BABU, G., & GHOSH, S. (2005) Geomorphic characterization and diversity of the
35
36 772 fluvial systems of the Gangetic Plains. *Geomorphology*, 70, 207-225.
- 37
38 773 SINHA, R., BHATTACHARJEE, P., SANGODE, S.J., GIBLING, M.R., TANDON, S.K., JAIN, M., & GODFREY, D.
39
40 774 (2007) Valley and interfluvial sediments in the southern Ganga plains, India: exploring facies and
41
42 775 magnetic signatures. *Sedimentary Geology*, 201, 386-411.
- 43
44
45 776 SINHA, R., GAURAV, K., CHANDRA, S., & TANDON, S.K. (2013) Exploring the channel connectivity structure
46
47 777 of the August 2008 avulsion belt of the Kosi River, India: application to flood risk assessment. *Geology*,
48
49 778 41, 1099-1102.
- 50
51 779 SINHA, R., AHMAD, J., GAURAV, K., & MORIN, G. (2014a) Shallow subsurface stratigraphy and alluvial
52
53 780 architecture of the Kosi and Gandak megafans in the Himalayan foreland basin, India. *Sedimentary*
54
55 781 *Geology*, 301, 133-149.
- 56
57
58
59
60

- 1
2 782 SINHA, R., SRIPRIYANKA, K., JAIN, V., AND MUKUL, M. (2014b) Avulsion threshold and planform dynamics of
3
4 783 the Kosi River in north Bihar (India) and Nepal. *Geomorphology*, 216, 157-170.
5
6 784 SINHA, S., SURESH, N., KUMAR, R., DUTTA, S. & ARORA, B.R. (2010) Sedimentologic and geomorphic studies
7
8 785 on the Quaternary alluvial fan and terrace deposits along the Ganga exit. *Quaternary International*,
9
10 786 227, 87-103
11
12 787 SRIVASTAVA, P., SINGH, I.B., SHARMA, M., & SINGHVI, A.K. (2003) Luminescence chronometry and Late
13
14 788 Quaternary geomorphic history of the Ganga Plain, India. *Palaeogeography, Palaeoclimatology,*
15
16 789 *Palaeoecology*, 197, 15-41.
17
18
19 790 SRIVASTAVA, P., TRIPATHI, J.K., ISLAM, R., & JAISWAL, M.K. (2008) Fashion and phases of late Pleistocene
20
21 791 aggradation and incision in the Alaknanda River Valley, western Himalaya, India. *Quaternary Research*,
22
23 792 70, 68-80.
24
25 793 TANDON, S.K., GIBLING, M.R., SINHA, R., SINGH, V., GHAZANFARI, P., DASGUPTA, A., JAIN, M., & JAIN, V.
26
27 794 (2006) Alluvial valleys of the Gangetic Plains, India: causes and timing of incision. In: *Incised Valleys in*
28
29 795 *Time and Space, SEPM Special Publication*, 85, 15-35.
30
31
32 796 TAYLOR, P.J., & MITCHELL, A.W. (2000) The Quaternary glacial history of the Zaskar range, north-west
33
34 797 Indian Himalaya. *Quaternary International*, 65, 81-99.
35
36 798 TAYLOR, M., & YIN, A. (2009) Active structures of the Himalayan-Tibetan orogeny and their relationships to
37
38 799 earthquake distribution, contemporary strain field, and Cenozoic volcanism. *Geosphere*, 5, 199-214.
39
40 800 THAKUR, V.C. (2013) Active tectonics of Himalayan Frontal Fault system. *International Journal of Earth*
41
42 801 *Science (Geol. Rundsch.)*, 102, 1791-1810.
43
44 802 THAKUR, V.C., & PANDEY, A.K. (2004) Late Quaternary tectonic evolution of Dun in fault bend/propagated
45
46 803 fold system, Garhwal Sub-Himalaya. *Current Science*, 87, 1567-1576.
47
48 804 THAKUR, V.C., PANDEY, A.K., & SURESH, N. (2007) Late Quaternary–Holocene evolution of Dun structure
49
50 805 and the Himalayan Frontal Fault zone of the Garhwal Sub-Himalaya, NW India. *J. Asian Earth Sci.*, 29,
51
52 806 305-319.
53
54
55 807 VANCE, D., BICKLE, M., IVY-OCHS, S., & KUBIK, P.W. (2003) Erosion and exhumation in the Himalaya from
56
57 808 cosmogenic isotope inventories of river sediments. *Earth and Planetary Science Letters*, 206, 273-288.
58
59
60

- 1
2 809 WALLING, D.E. (1983) The sediment delivery problem. *Journal of Hydrology*, 65, 209-237.
3
4 810 WASSON, R.J. (2003) A sediment budget for the Ganga-Brahmaputra catchment. *Current Science*, 84, 1041-
5
6 811 1047.
7
8 812 WESNOUSKY, S.G., KUMAR, S., MOHINDRA, R., & THAKUR, V.C. (1999) Uplift and convergence along the
9
10 813 Himalayan Frontal thrust of India. *Tectonics*, 18, 967-976.
11
12 814 WICKERT, A.D., MARTIN, J.M., TAL, M., KIM, W., SHEETS, B., & PAOLA, C. (2013) River channel lateral
13
14 815 mobility: metrics, time scales, and controls. *Journal of Geophysical Research – Earth Surface*, 118,
15
16 816 10.1029/2012JF002386.
17
18 817 YEATS, R.S., & LILLIE, R.J. (1991) Contemporary tectonics of the Himalayan frontal fault system: folds, blind
19
20 818 thrusts and the 1905 Kangra earthquake. *J. Structural Geol.*, 13, 215-225.
21
22 819 YEATS, R.S., NAKATA, T., FARAH, A., FORT, M., MIRZA, M.A., PANDEY, M.R., & STEIN, R.S. (1992) The
23
24 820 Himalayan frontal fault system. *Annales Tectonicae, Spec. Issue, Suppl. to Vol. VI*, 85-98.
25
26
27
28
29
30
31
32
33
34
35
36
37
38
39
40
41
42
43
44
45
46
47
48
49
50
51
52
53
54
55
56
57
58
59
60

Figure Captions

- 1
2 821 **Figure Captions**
3
4 822 1. Location map showing major rivers (white) and duns along the Himalayan mountain front, India and
5
6 823 Nepal. Heavy black lines show simplified trace of the Main Boundary Thrust (MBT) and Himalayan Frontal
7
8 824 Thrust (HFT) fault systems, while light shaded areas highlight the region between the MBT and HFT where
9
10 825 the major duns are developed. Barbs on faults mark the upthrown block. Faults simplified from Yeats et al.
11
12 826 (1992) and Taylor and Yin (2009). White boxes show the locations of the three regions discussed here.
13
14 827
15
16 828 2. A, Overview and geomorphic map of the Dehra Dun area, overlain on a hillshade image of the SRTM
17
18 829 DEM. MBT, Main Boundary Thrust system; HFT, Himalayan Frontal Thrust system. Heavy white lines show
19
20 830 the Ganga and Yamuna catchments, while white shaded areas indicate the Catchments that flow into the
21
22 831 dun. Holocene terrace deposits are shown in pale yellow; those along the Yamuna River are taken from
23
24 832 Dutta et al. (2012), while those along the Ganga River are taken from Sinha et al. (2010). DO, DD, and BP
25
26 833 mark the Donga, Dehradun, and Bhogpur fans of Singh et al. (2001). B, Depositional units on the Donga and
27
28 834 Dehradun fans. Our analysis is focused on the isolated hills, proximal fan, and distal fan units. SF,
29
30 835 Santaugarh fault. White circles mark OSL ages determined in this study, while grey circles mark ages
31
32 836 published by Singh et al. (2001); sample positions, ages, and depths below surface are given in Table 1. Red
33
34 837 dots mark locations of boreholes used to establish minimum fan deposit thicknesses. Eye symbols in
35
36 838 hangingwall of Santaugarh fault show viewpoints of photos in Fig. 3.
37
38 839
39
40 840 3. Relationships between depositional units near the headwaters of the Koti Nadi, in the hangingwall of the
41
42 841 Santaugarh fault. See Fig. 2 for locations. A, Deposits of the isolated hills unit unconformably overlie Middle
43
44 842 Siwalik rocks in the fault hangingwall; in turn, both of these units are unconformably draped by the
45
46 843 proximal fan unit. View is to the west-southwest. The near-planar surface of the proximal fan unit is clearly
47
48 844 visible, and can be traced continuously across the Santaugarh fault (out of the photo to the left) on the
49
50 845 south bank of the Koti Nadi. B, spatial changes in sediment transport direction recorded in the walls of the
51
52 846 Koti Nadi. View is to the east. Deposits of the proximal fan unit are separated from the underlying isolated
53
54 847 hills unit by an angular uniformity that marks the margin of a paleovalley incised into the isolated hills unit.
55
56
57
58
59
60

1
2 848 Subsequently, the proximal fan unit was abandoned and incised, and the new valley trends more westerly
3
4 849 (toward the camera).

5
6 850

7
8 851 4. Estimated depth of incision into the proximal fan unit on the Donga (DO) and Dehradun (DD) fans.

9
10 852 Orange areas show the mapped extents of the proximal fan unit that were used to interpolate the likely

11
12 853 original depositional extent. Shading indicates the depth of incision, which reaches ~180 m near the

13
14 854 headwaters of the major valleys, particularly the Suarna and Asan rivers, and tapers to 0 downstream. This

15
16 855 is equivalent to the removal of 1900 Mm³ of sediment from the Donga fan and 750 Mm³ from the

17
18 856 Dehradun fan since abandonment of the proximal fan unit.

19
20
21 857

22
23 858

24
25 859 5. Overview of the Chitwan Dun area, overlain on a hillshade image of the SRTM DEM. The dun is formed

26
27 860 between strands of the Main Boundary Thrust (MBT) and Main Dun Thrust (MDT) fault systems to the

28
29 861 north, and the Himalayan Frontal Thrust (HFT) system to the south. Faults are simplified from Lave and

30
31 862 Avouac (2001). The Gandak River enters the dun at Narayangarh and flows west-southwest across the dun,

32
33 863 eventually crossing the HFT at Tribeni and flowing into the foreland. The Bishannagar-Kirtipur (yellow) and

34
35 864 Barakot-Belani (orange) depositional units of Kimura (1995) are preserved along the northern margin of the

36
37 865 dun, in the footwall of the MDT. Shading indicates the depth of incision into the more widespread

38
39 866 Bishannagar-Kirtipur unit, which reaches ~70 m in the immediate fault footwall and tapers to the south.

40
41
42 867

43
44 868 6. Overview of the Kosi River exit. Background is Landsat 7 ETM+ image with band combination 732. Faults

45
46 869 are simplified from Lave and Avouac (2000, 2001). The Kosi flows across strands of the MBT and HFT and

47
48 870 enters the foreland at Chatra. High sediment supply and frequent avulsions by the Kosi have constructed a

49
50 871 broad sediment fan in the foreland; several south-draining palaeochannels are visible in the image.

51
52
53 872

54
55 873 7. Conceptual model of sediment supply to the foreland in the presence (A, B) and absence (C) of a dun.

56
57 874 Insets show hypothetical evolution of sediment discharge into ($Q_{s\ in}$) and out of ($Q_{s\ out}$) the dun in the face of

1
2 875 externally-imposed variations in climate and sediment supply. A, Mountain front evolution during times of
3
4 876 sediment accumulation within the dun, such that $Q_{s\ in} > Q_{s\ out}$. This mismatch could arise due to some
5
6 877 combination of low or increasing sediment supply from the hinterland, low transport capacity in the
7
8 878 system, or both. Deformation is distributed between active faults on the upstream and downstream
9
10 879 margins of the dun, leading to moderate rates of rock uplift and incision above individual structures. The
11
12 880 dun provides accommodation for sediment from both local river systems and large-scale hinterland rivers.
13
14 881 Fan deposition in the dun acts as a partial, transient sediment trap until the dun fills, at which point the dun
15
16 882 can be bypassed and sediment discharge to the foreland $Q_{s\ out}$ may rise (inset). This phase represents
17
18 883 aggradation in the dun observed during 41-33 and 23-16 ka. B, Mountain front evolution during times of
19
20 884 sediment evacuation from the dun, such that $Q_{s\ in} < Q_{s\ out}$. The mismatch could arise due to some
21
22 885 combination of high sediment supply from the hinterland, high or increasing transport capacity, or both.
23
24 886 Fan incision and sediment evacuation from the dun is likely to cause an increase in $Q_{s\ out}$ (inset). This phase
25
26 887 represents incision in the dun observed since 10 ka. C, Mountain front evolution in the absence of a dun.
27
28 888 Deformation is concentrated at the thrust front, leading to rapid rock uplift of recycled, easily-erodible
29
30 889 foreland basin deposits and high rates of sediment supply from the immediate fault hangingwall. The
31
32 890 addition of this eroded material means that the sediment discharge to the foreland $Q_{s\ out}$ is greater than the
33
34 891 sediment discharge delivered to the immediate hangingwall $Q_{s\ in}$. The lack of intermediate storage leads to
35
36 892 efficient export of sediment to the foreland, so that $Q_{s\ out}$ tracks $Q_{s\ in}$ closely (inset).
37
38
39
40
41
42
43
44
45
46
47
48
49
50
51
52
53
54
55
56
57
58
59
60

Table 1. OSL samples and analytical results

Sample (Lab code)	Depo. unit	Position	Elev. (m)	Depth (m) ^a	U (ppm)	Th (ppm)	K (%)	Moist. cont. (%)	Equivalent dose De (Gy)		Dose rate (Gy/ka)	Age (ka)	
									Weighted mean	Least		Weighted mean	Least
FS2.1 (LD1040)	Distal fan	30° 24' 20.4" 77° 56' 55.5"	790	4	2.23±0.02	15.3±0.15	2.91±0.03	3.44	59.68±3.96	45.26±3.41	4.33±0.05	13.8±0.9	10.5±0.8
FS2.2 (LD1041)	Distal fan	30° 26' 41.9" 77° 51' 35.5"	618	5	2.43±0.02	16±0.16	2.46±0.02	13.53	51.46±1.87	44.36±5.44	3.58±0.06	14.4±0.6	12.4±1.5
LIS-TOP (LD1147)	Distal fan	30° 24' 18.9" 77° 56' 56.8"	789	2.8	3.3±0.03	18.1±0.18	3.02±0.03	1.27	80.72±6.82	72.23±7.62	4.99±0.06	16.2±1.4	14.5±1.5
FS3.1 (LD1042)	Proximal fan	30° 24' 46.7" 77° 57' 35.3"	855	10	1.89±0.02	16.4±0.16	2.21±0.02	18.16	65.71±3.62	66.36±3.8	3.10±0.06	21.2±1.3	21.4±1.3
FS1.1 (LD1039)	Proximal fan	30° 21' 39.6" 77° 56' 28.6"	606	3	4.56±0.05	21.4±0.21	2.65±0.03	14.38	150.87±14.2	128.9±15.4	4.47±0.08	33.8±3.2	28.8±3.5
IH/2 (LD1148)	Isolated hills	30° 24' 46.2" 77° 57' 29.7"	843	2.8	3.1±0.03	18.4±0.18	3.08±0.03	1.36	207.20±5.47	208.6±6.2	5.02±0.06	41.3±1.2	41.6±1.3

^a Depth below surface of depositional unit, in m

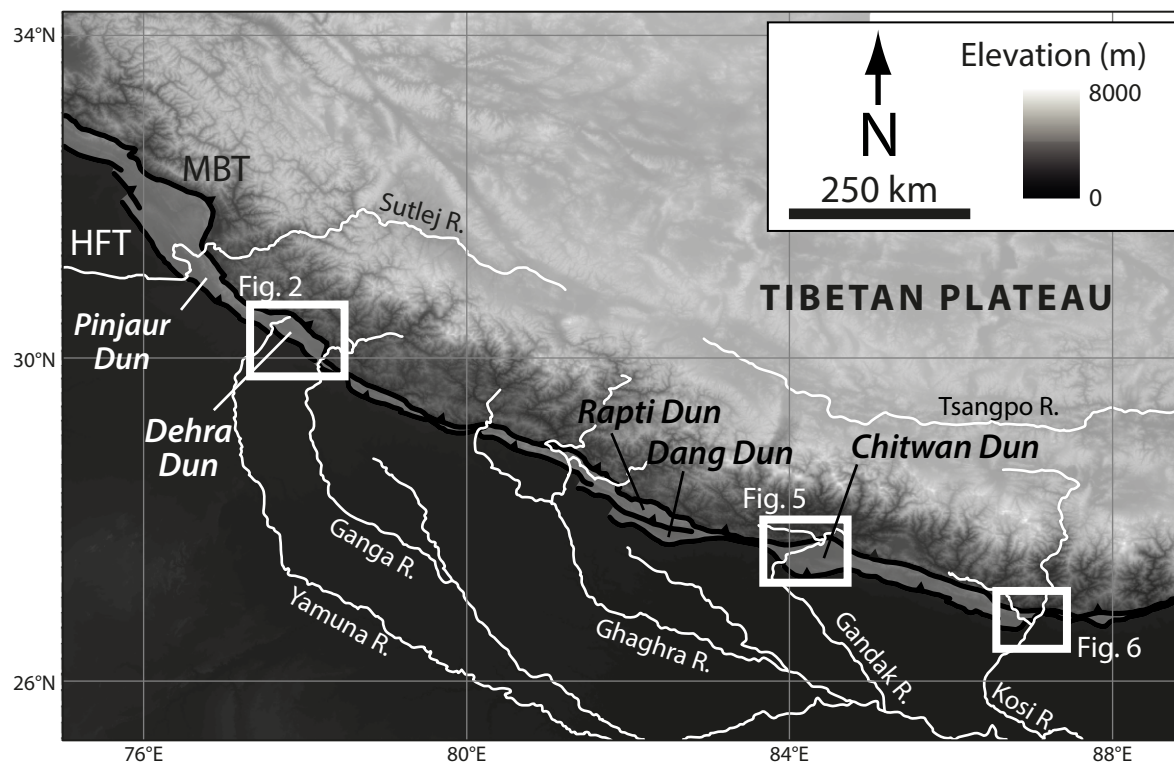
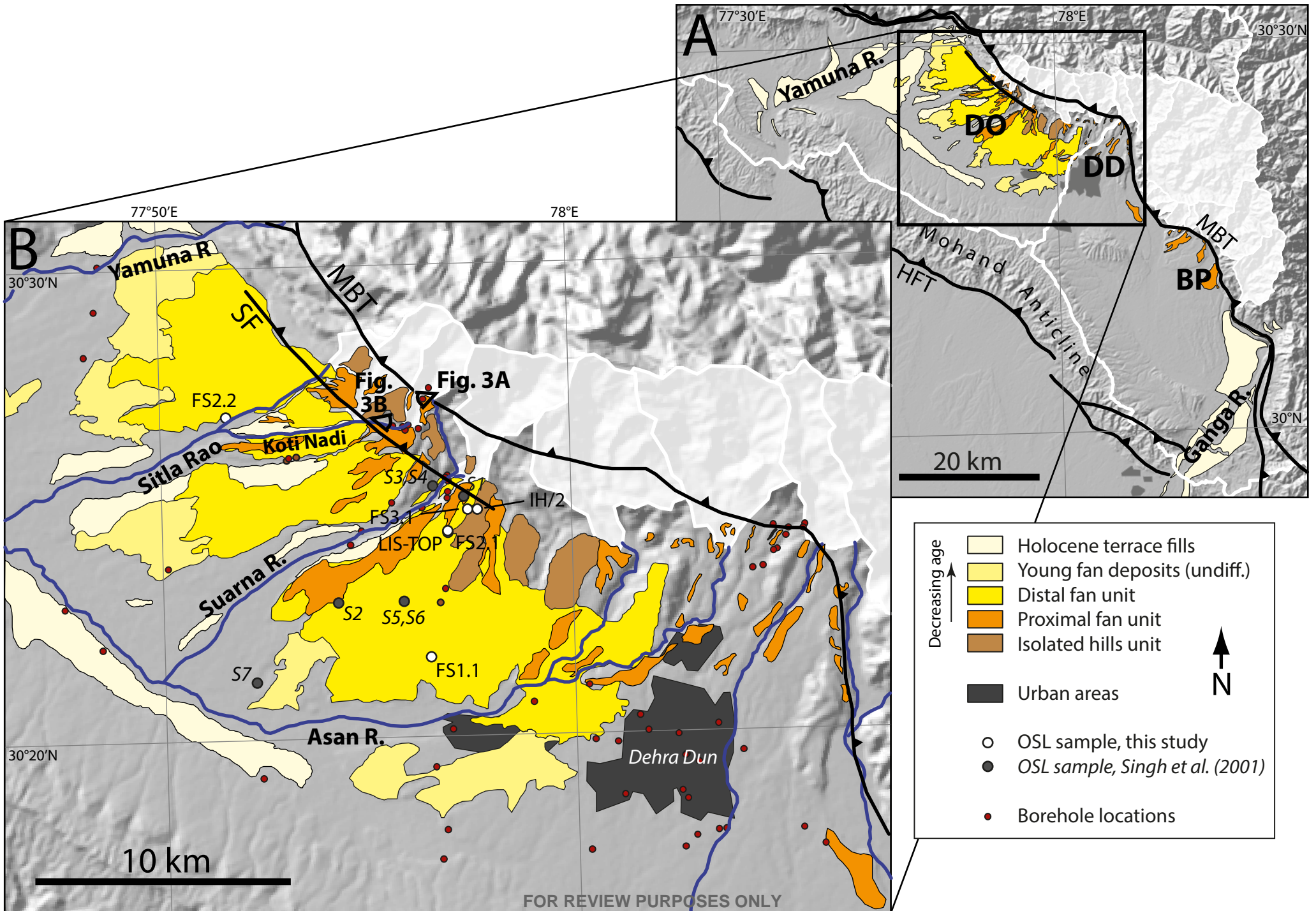
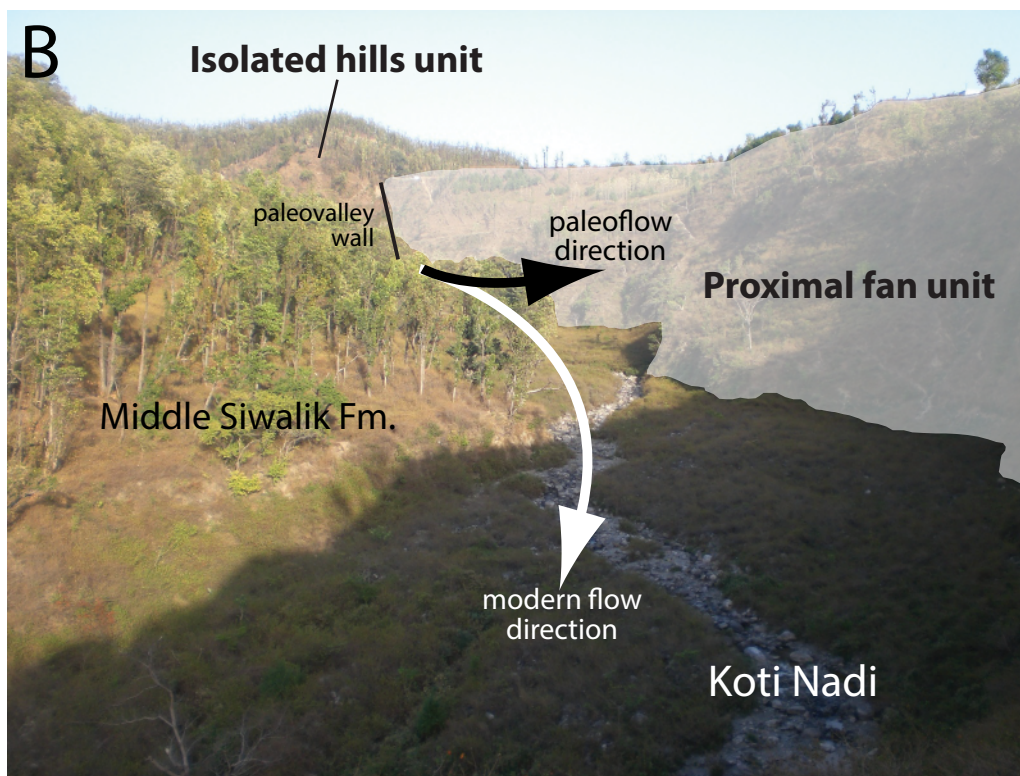
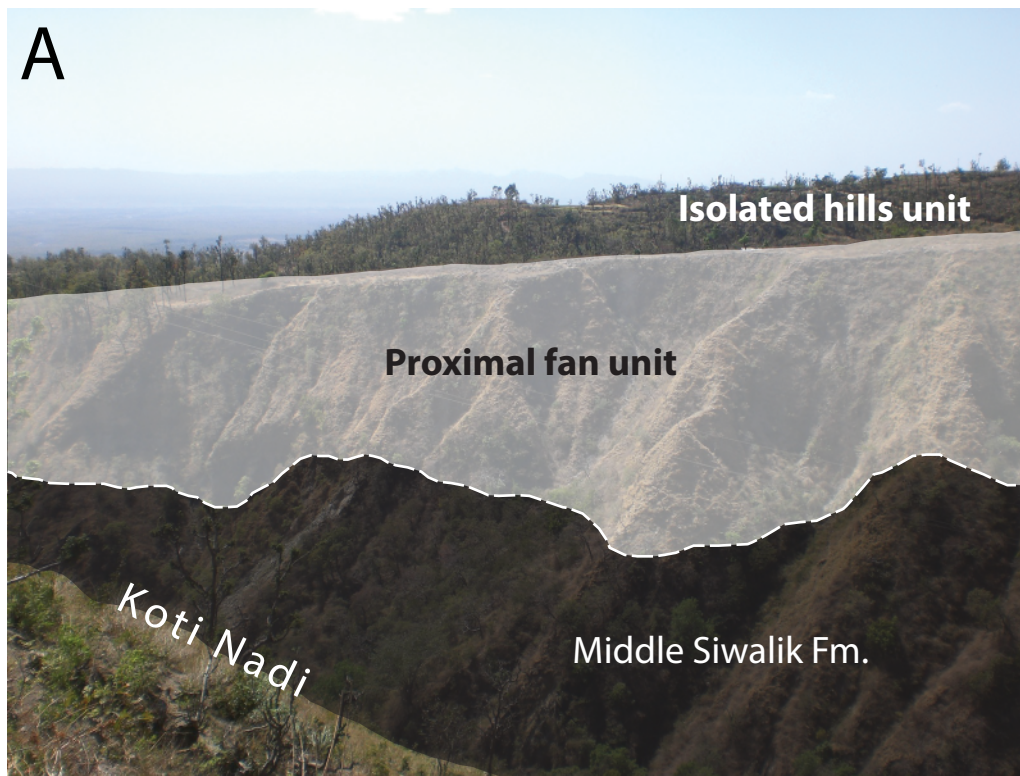


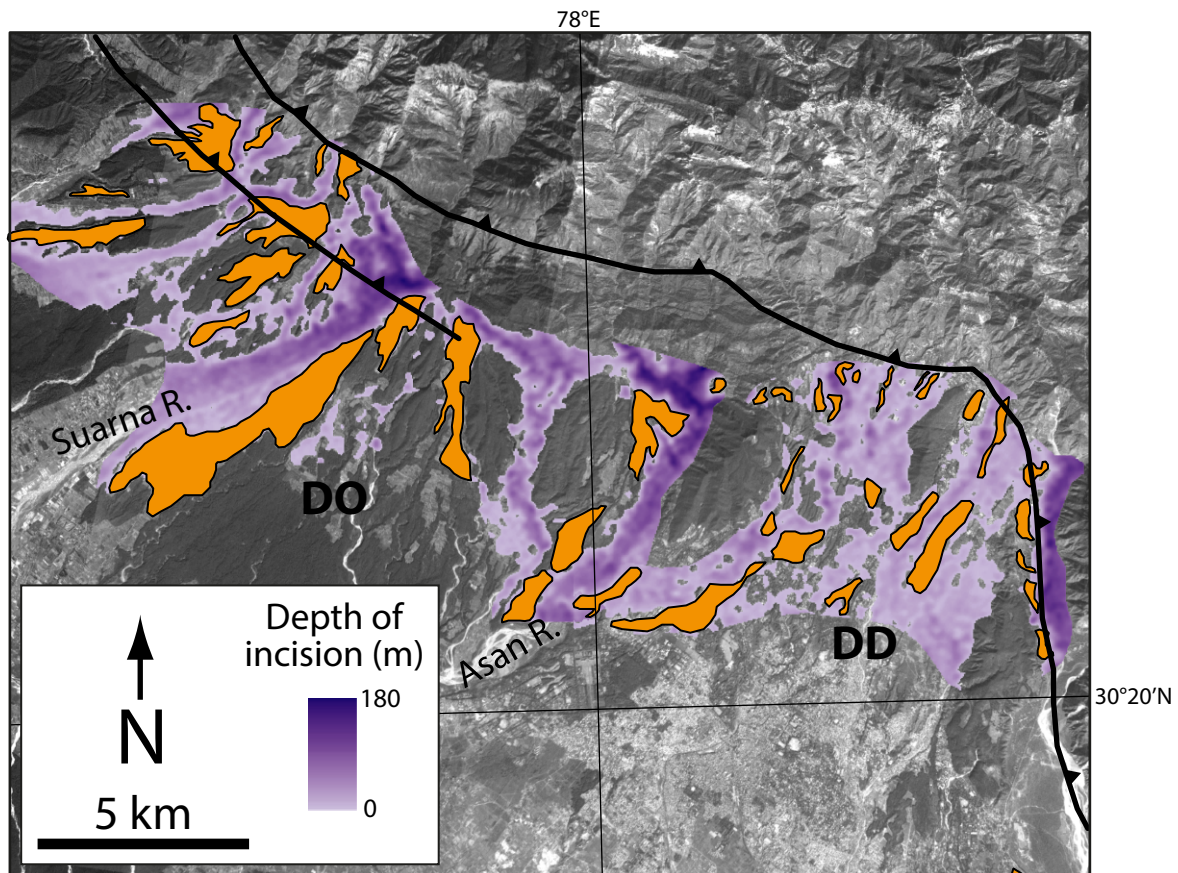
Fig. 1. Location map showing major rivers (white) and duns along the Himalayan mountain front, India and Nepal. Heavy black lines show simplified traces of the Main Boundary Thrust (MBT) and Himalayan Frontal Thrust (HFT) fault systems, while light shaded areas highlight the region between the MBT and HFT where the major duns are developed. Barbs on faults mark the upthrust block. Faults are simplified from Yeats et al. (1992) and Taylor and Yin (2009). White boxes show the locations of the three regions discussed here.



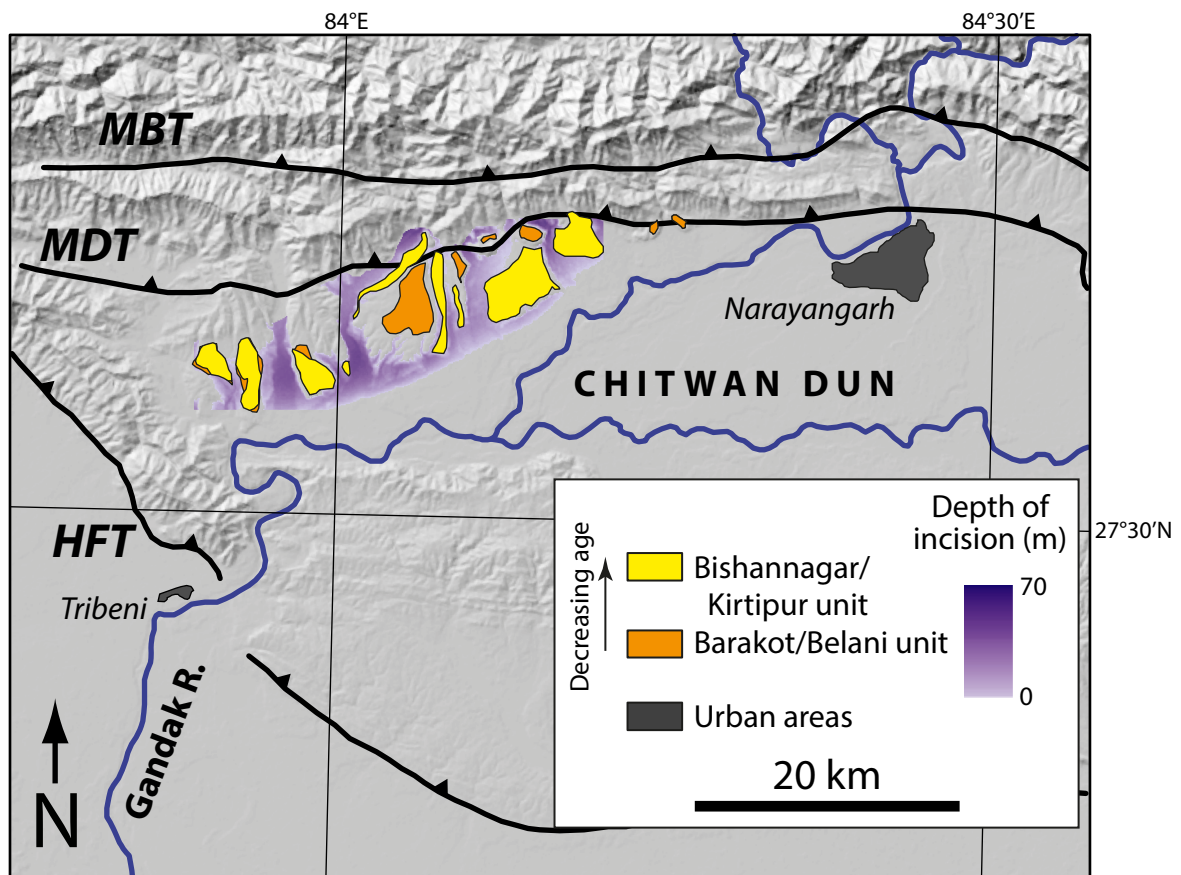
1
2
3
4
5
6
7
8
9
10
11
12
13
14
15
16
17
18
19
20
21
22
23
24
25
26
27
28
29
30
31
32
33
34
35
36
37
38
39
40
41
42
43
44
45
46
47



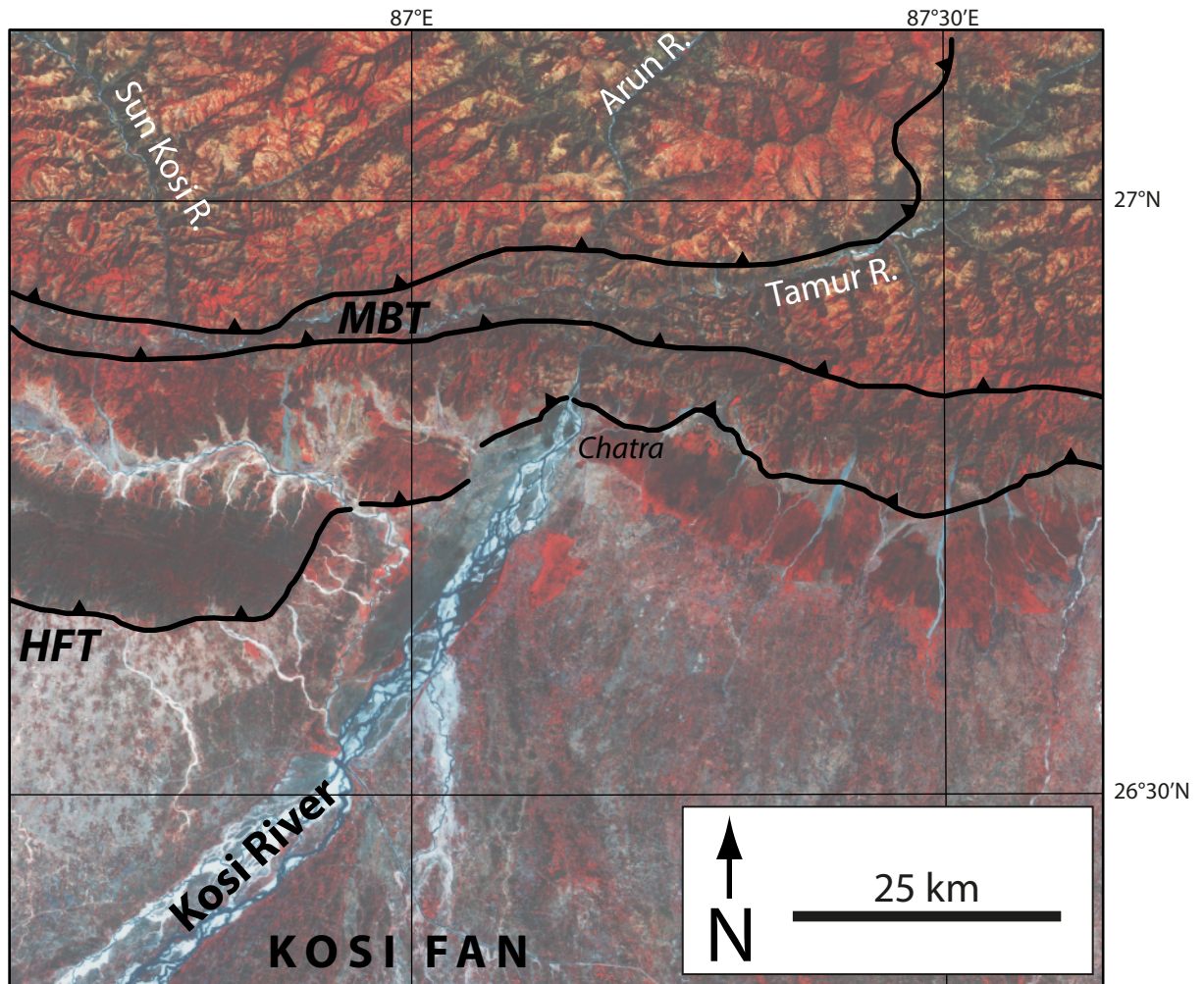
53 3. Relationships between depositional units near the headwaters of the Koti Nadi, in the hangingwall of the Santaugarh
 54 fault. See Fig. 2 for locations. A, Deposits of the isolated hills unit unconformably overlie Middle Siwalik rocks in the fault
 55 hangingwall; in turn, both of these units are unconformably overlain draped by the proximal fan unit. View is to the west-
 56 southwest. The near-planar surface of the proximal fan unit is clearly visible, and can be traced continuously across the
 57 Santaugarh fault (out of the photo to the left) on the south bank of the Koti Nadi. B, spatial changes in sediment transport
 58 direction recorded in the walls of the Koti Nadi. View is to the east. Deposits of the proximal fan unit are separated from the
 59 underlying isolated hills unit by an angular unconformity that marks the margin of a paleovalley incised into the isolated hills
 60 unit. Subsequently, the proximal hills fan unit was abandoned and incised, and the new valley trends more westerly
 (toward the camera).



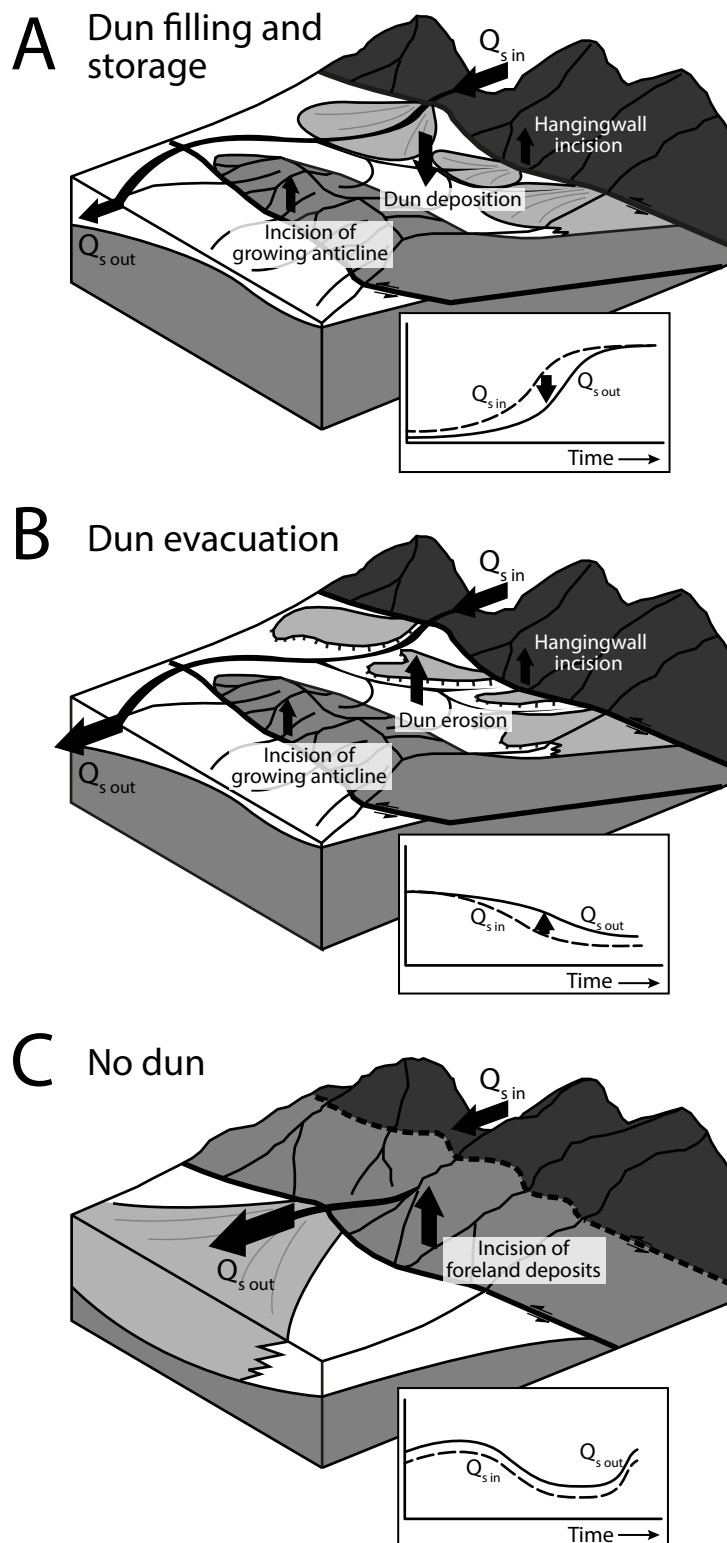
4. Estimated depth of incision into the proximal fan unit on the Donga (DO) and Dehradun (DD) fans. Orange areas show the mapped extents of the proximal fan unit that were used to interpolate the likely original depositional extent. Shading indicates the depth of incision, which reaches ~180 m near the headwaters of the major valleys, particularly the Suarna and Asan rivers, and tapers to 0 downstream. This is equivalent to the removal of 1900 Mm³ of sediment from the Donga fan and 750 Mm³ from the Dehradun fan since abandonment of the proximal fan unit.



5. Overview of the Chitwan Dun area, overlain on a hillshade image of the SRTM DEM. The dun is formed between strands of the Main Boundary Thrust (MBT) and Main Dun Thrust (MDT) fault systems to the north, and the Himalayan Frontal Thrust (HFT) system to the south. Faults are simplified from Lave and Avouac (2001). The Gandak River enters the dun at Narayangarh and flows west-southwest across the dun, eventually crossing the HFT at Tribeni and flowing into the foreland. The Bishannagar-Kirtipur (yellow) and Barakot-Belani (orange) depositional units of Kimura (1995) are preserved along the northern margin of the dun, in the footwall of the MDT. Shading indicates the depth of incision into the more widespread Bishannagar-Kirtipur unit, which reaches ~70 m in the immediate fault footwall and tapers to the south.



6. Overview of the Kosi River exit. Background is Landsat 7 ETM+ image from XXX, with band combination 732 . Faults are simplified from Lave and Avouac (2000, 2001). The Kosi flows across strands of the MBT and HFT and enters the foreland at Chatra. High sediment supply and frequent avulsions by the Kosi have constructed a broad sediment fan in the foreland; several south-draining palaeochannels are visible in the image.



7. Conceptual model of sediment supply to the foreland in the presence (A, B) and absence (C) of a dun. Insets show hypothetical evolution of sediment discharge into ($Q_{s\ in}$) and out of ($Q_{s\ out}$) the dun in the face of externally-imposed variations in climate and sediment supply. A, Mountain front evolution during times of sediment accumulation within the dun, such that $Q_{s\ in} > Q_{s\ out}$. This mismatch could arise due to some combination of increasing sediment supply from the hinterland, decreasing transport capacity in the system, or both. Deformation is distributed between active faults on the upstream and downstream margins of the dun, leading to moderate rates of rock uplift and incision above individual structures. The dun provides accommodation for sediment from both local river systems and large-scale hinterland rivers. Fan deposition in the dun acts as a partial, transient sediment trap until the dun fills, at which point the dun can be bypassed and sediment discharge to the foreland $Q_{s\ out}$ may rise (inset). This phase represents aggradation in the dun observed during 41-33 and 23-16 ka. B, Mountain front evolution during times of sediment evacuation from the dun, such that $Q_{s\ in} < Q_{s\ out}$. The mismatch could arise due to some combination of decreasing sediment supply from the hinterland, increasing transport capacity, or both. Fan incision and sediment evacuation from the dun is likely to cause an increase in $Q_{s\ out}$ (inset). This phase represents incision in the dun observed since 10 ka. C, Mountain front evolution in the absence of a dun. Deformation is concentrated at the thrust front, leading to rapid rock uplift of recycled, easily-erodible foreland basin deposits and high rates of sediment supply from the immediate fault hangingwall. The addition of this eroded material means that the sediment discharge to the foreland $Q_{s\ out}$ is greater than the sediment discharge delivered to the immediate hangingwall $Q_{s\ in}$. The lack of intermediate storage leads to efficient efflux of sediment to the foreland, so that $Q_{s\ out}$ tracks $Q_{s\ in}$ closely (inset).

1
2 **Sediment storage and release from Himalayan piggyback basins and implications for downstream river**
3
4 **morphology and evolution**

5
6
7
8 **Supplementary Material**
9

10
11
12 **Optically-stimulated luminescence dating: sampling and analytical details**

13
14 The sediment samples collected from depositional units in the Dehra Dun were dated using luminescence
15 dating techniques. Samples were collected in plastic pipes and immediately sealed in black, lightproof
16 plastic bags to prevent exposure to light.
17
18
19

20
21
22
23 In the laboratory, under subdued red light conditions, sample material from the middle part of the pipe
24 was transferred to a beaker and treated with 1N HCl and 30% H₂O₂ to remove carbonate and organic
25 matter, respectively. After treatment, the material was sieved to obtain the 90-125 µm size fraction
26 (Aitken, 1985). Quartz grains (with an assumed density of 2.65 g/cm³) were extracted from this size fraction
27 by density separation using sodium polytungstate solution. The extracted quartz grains were etched for 80
28 minutes in 40% hydrofluoric acid (HF) to remove the outer layer from each grain, treated with HCl and
29 washed in distilled water, and then re-sieved using a 200 mesh (75 µm) sieve. The HF treatment also
30 served to remove any feldspar contamination. The purity of the etched quartz and the lack of feldspar
31 contamination was verified by infra-red stimulated luminescence (IRSL). The values obtained were low for
32 all samples, suggesting negligible feldspar contamination (Suppl. Fig. S1).
33
34
35
36
37
38
39
40
41
42
43
44
45
46

47 The etched quartz grains were then fixed into the centre of 10 mm diameter stainless steel discs to form a
48 3 mm diameter monolayer, using silicon oil as the adhesive agent. Between 35 and 39 aliquots were
49 prepared per sample, and the Single Aliquot Regeneration (SAR) protocol (Murray and Wintle, 2000) was
50 used to determine the radiation energy received by the sample after its burial, also known as the
51 equivalent dose (De). Optically Stimulated Luminescence (OSL) measurements were carried out on an
52 automated Risø TL/DA 20 reader (Risø Laboratories, Denmark) equipped with a blue LED light source for
53
54
55
56
57
58
59
60

1 stimulation, using the following measurement settings: pre-heat 240°C, cut-heat 160°C, test dose ~15% of
2 expected D_e , blue light stimulation 40 s and Hoya U-340 detection filters.
3
4

5
6
7
8 In the SAR protocol, the same aliquot is subjected to a series of cycles of measurements and the resulting
9 sensitivity changes (due to repeated heating during measurement cycles) were normalized by a test dose
10 signal. We first measured the natural luminescence (L_n) using 240°C pre-heat and 40 s blue light
11 stimulation at 125°C, followed by the test dose luminescence signal (T_n) using 160°C cut heat and 40 sec
12 blue light stimulation at 125°C for sensitivity correction. Subsequently, the regenerated luminescence
13 signals were generated by applying different irradiation doses ($L\beta_1$, $L\beta_2$, $L\beta_3$, $L\beta_0$ and $L\beta_1$), along with the
14 corresponding test dose signals. Estimates of D_e were achieved by comparing the natural luminescence
15 signal with those induced by laboratory irradiation, and the regenerated growth curve for each sample was
16 constructed using Duller's Analyst software, using an exponential fit for D_e calculation. This was done using
17 the test dose value normalized fast component of the OSL (initial integral of 0.8 s) and the regenerated
18 signals. The shine down curves (OSL intensity plotted as a function of light stimulation) and representative
19 regenerated growth curves for samples LD1039-LD1042, LD1147, and LD1148 are shown in Suppl. Fig. S2.
20
21 The disc-to-disc scatter (5–10%) is typical of that observed in quartz OSL measurement (Smith et al., 1990).
22
23 The quartz shine down curve shows how the luminescence emitted by the mineral grains evolves as the
24 electrons in the traps are emptied, rapidly for the first few seconds and then at a decaying rate. The growth
25 curve is used to determine the laboratory dose that regenerates a luminescence signal that matches the
26 intensity of the natural luminescence signal in the sample.
27
28
29
30
31
32
33
34
35
36
37
38
39
40
41
42
43
44

45
46 Additional aliquots were prepared for sample LD1039 to conduct a dose recovery test. The aliquots were
47 first bleached (similar to natural bleaching) for 100 sec by blue LED stimulation and a known quantity
48 (133.33 Gy) of dose was applied using the calibrated beta source (Sr/Yr^{90}) in the instrument. The given dose
49 was recovered using the SAR protocol. The dose recovery test was carried out at various pre-heat
50 temperatures (200, 220, 240 and 260°C), showing that the recovered value is always within error limits and
51 does not show any systematic changes with pre-heat temperatures, and hence documenting the thermal
52 stability of the quartz signal (pre-heat plateau). The results of the dose recovery test for this sample are
53
54
55
56
57
58
59
60

1 shown in Suppl. Fig. S3.
2
3
4
5

6 Our samples show a wide distribution of De values, perhaps due to partial bleaching during transportation.
7
8 Thus, the abnormally high De values were omitted from subsequent calculations, and the De value was
9
10 obtained from between 8 and 20 aliquots (out of 35-39 per sample). For the annual dose rate estimation,
11
12 the concentrations of uranium, thorium and potassium in the samples were measured by XRF and the
13
14 water content was determined by heating at 100°C. No measurements for cosmic ray contribution were
15
16 carried out. The ages were calculated using AGE (Grun, 2009), which uses the depth of the sample below
17
18 the surface to determine the cosmic dose rate, assuming a sediment density of 2000 kg/m³ using a
19
20 standard value of 150 µ Gy. The ages were calculated using the weighted mean of De divided by the dose
21
22 rate value. We argue that the weighted mean is a better estimate of age as it will depend upon the actual
23
24 distribution of De values. However, we have provided the least De values and associated ages in Table 1.
25
26
27
28
29

30 **References**

- 31
32 AITKEN, M.J. (1985) *Thermoluminescence Dating*, Academic Press, London, 359 pp.
33
34 GRUN, R. (2009) The 'AGE' program for the calculation of luminescence age estimates. *Ancient TL*, 27, 45-
35
36 46.
37
38 MURRAY, A.S. & WINTLE, A.G. (2000) Luminescence dating of quartz using an improved single-aliquot
39
40 regenerative-dose protocol. *Radiation Measurements*, 32, 57-73.
41
42 SMITH, B.W., RHODES, E.J., STOKES, S., SPOONER, N.A., & AITKEN, M.J. (1990) Optical dating of sediments:
43
44 initial quartz results from Oxford. *Archaeometry*, 32, 19-31.
45
46
47
48
49
50
51
52
53
54
55
56
57
58
59
60

Supplementary Figures

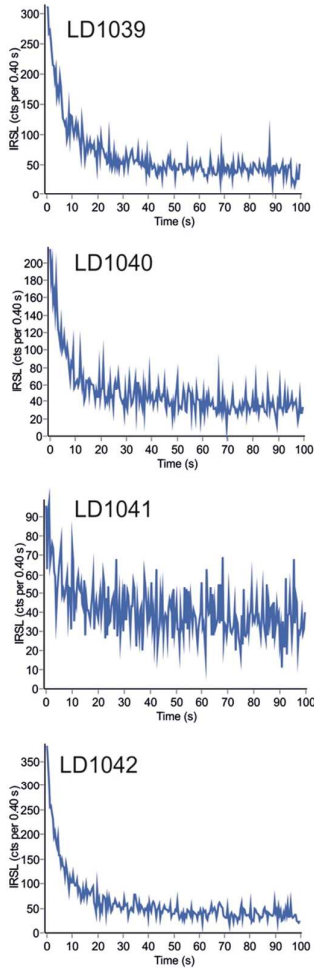


Fig. S1. IRSL signal for samples LD1039 to LD1042. Low values of the IRSL signal suggest that feldspar contamination in the samples is negligible.

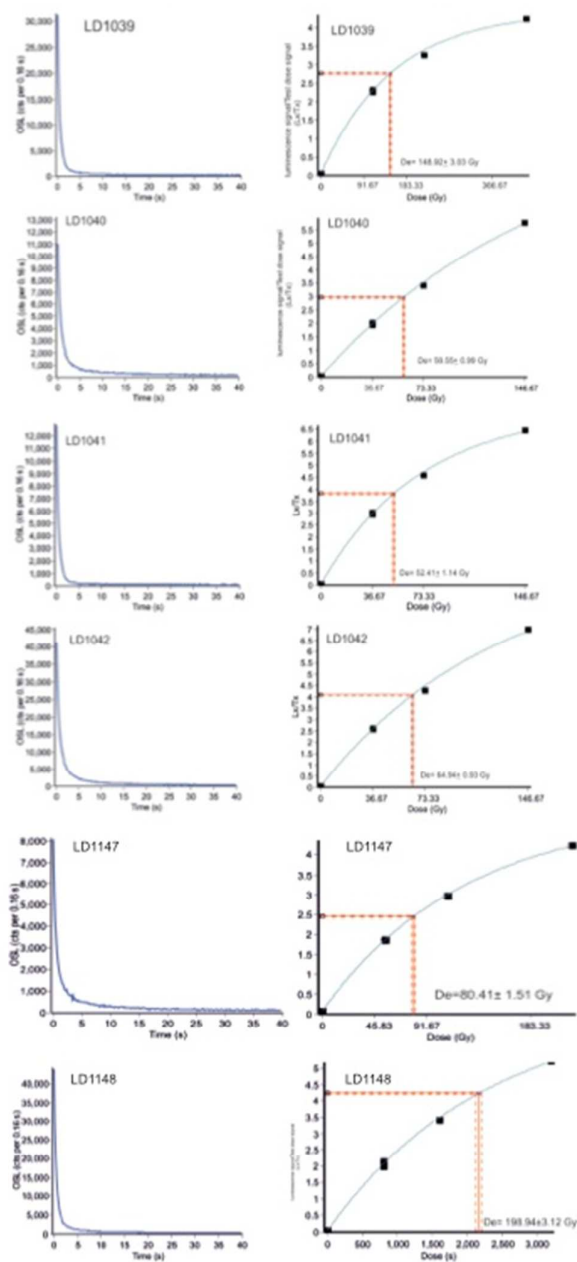
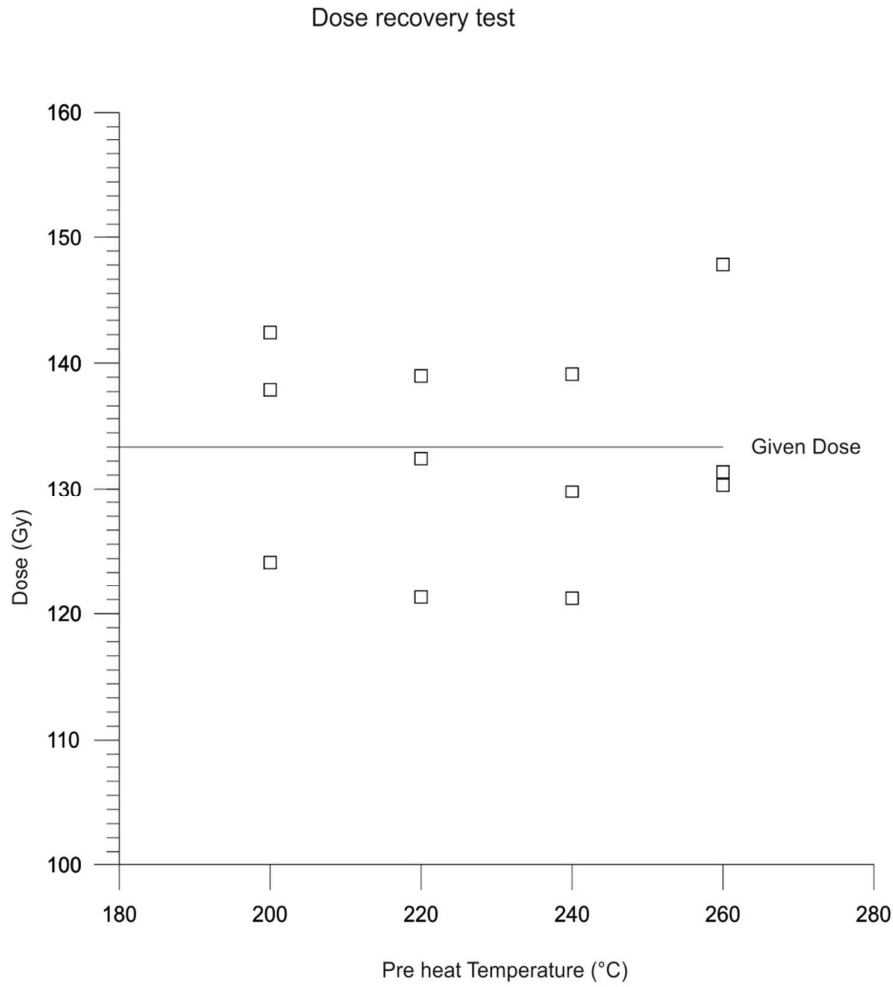


Fig. S2. Shine down curves (equivalent dose versus stimulation time, left panels) and regenerated growth curves (test dose normalized luminescence intensity versus laboratory beta dose, right panels) for equivalent dose determinations for samples LD1039 to LD1042, LD1147, and LD1148.



37
38
39
40
41
42
43
44
45
46
47
48
49
50
51
52
53
54
55
56
57
58
59
60

Fig. S3. Results of dose recovery test for sample LD1039. The applied beta dose (133.33 Gy) was successfully recovered using quartz SAR protocol. The test was carried out at various pre-heat temperatures (200, 220, 240, and 260°C), which shows the thermal stability of the quartz OSL signal and the suitability of the material for OSL dating.